HYDROGEN POSITIONS IN COLEMANITE

THE POSITIONS OF THE HYDROGEN ATOMS AND THEIR ROLE IN THE FERROELECTRIC BEHAVIOR OF COLEMANITE

by

FREDERIC NOEL HAINSWORTH, B.Sc., M.Sc.

A Thesis
Submitted to the Faculty of Graduate Studies
in Partial Fulfilment of the Requirements
for the Degree
Doctor of Philosophy

McMaster University
May 1965

DOCTOR OF PHILOSOPHY (1965)
Physics

McMASTER UNIVERSITY
Hamilton, Ontario

TITLE: The Positions of the Hydrogen Atoms and Their Role in the Ferroelectric Behavior of Colemanite

AUTHOR: Frederic Noel Hainsworth, B.Sc. (Queen's University)
M.Sc. (Queen's University)

SUPERVISOR: Professor H. E. Petch

NUMBER OF PAGES:

SCOPE AND CONTENTS: A neutron diffraction study of the hydrated borate mineral, colemanite ($CaB_3O_4(OH)_3 \cdot H_2O$) has been carried out at room temperature and at -20°C, primarily to determine the positions of the hydrogen atoms above and below the ferroelectric transition temperature of -2.5°C. Most of the hydrogen bonds in colemanite are of quite normal character and do not change appreciably through the transition. However, one of the hydrogen atoms of the water molecule and the hydrogen atom of an adjacent hydroxyl group, which are in a state of dynamic disorder at room temperature, are found to settle into ordered, non-centrosymmetric positions below the Curie point. Some of the other atoms are found to undergo small, but in some cases significant, displacements from their room temperature positions. Assuming a reasonable distribution of charges, the magnitude of the spontaneous polarization calculated from the observed positional changes is comparable to the measured value. These results have been used to develop a qualitative theory of the mechanism of the transition from the atomistic point of view.

ACKNOWLEDGEMENTS

The author is primarily indebted to Professor H. E. Petch for initiating this project and for his help and advice, especially towards the conclusion of the work. I am very grateful to all members of the crystallography group headed by Professors C. Calvo and I. D. Brown for their computer programs and many useful discussions.

Professor Petch and the author acknowledge the generosity of Mr. P. E. Desautels of the Smithsonian Institution for providing the excellent specimen of colemanite used in this study.

The author is grateful for the computer programs of Dr. W. C. Hamilton and of Drs. W. R. Busing, K. O. Martin and H. A. Levy, without which the data refinement would have been a formidable task.

This research has been supported by the National Research Council. The author is grateful to the Ontario Government and the National Research Council for personal financial support.

TABLE OF CONTENTS

Page

LIST OF FIGURES

LIST OF TABLES

I. INTRODUCTION

The first sample of the borate mineral, later to be known as colemanite was discovered in Death Valley, Inyo County, California in 1882. It has since been found in the presence of other borate deposits in Turkey, the U.S.S.R., and Argentina. The commercially-useful chemical, borax ($Na_2B_4O_7.10H_2O$), is easily derived from colemanite ($CaB_3O_4(OH)_3.H_2O$), and the latter was extensively mined for this purpose until the discovery of kernite ($Na_2B_4O_7.4H_2O$) in 1927. The industrial interest in colemanite then gradually diminished.

Its special dielectric properties were not discovered until 1956, although museum curators, noticing dust gathering preferentially on certain edges of colemanite specimen crystals, suspected pyroelectric properties. In the first study related to this matter, Davisson (1956) reported that the dielectric breakdown paths at room temperature and 150°C indicated that colemanite is centrosymmetric, with point group 2/m and hence should not be pyroelectric. The patterns at -195°C led him to believe that the crystal was basically centrosymmetric with possibly slight deviations. However, he also performed direct pyroelectric tests which showed a high, narrow anomaly in the pyroelectric activity at -2.5°C with a long tail extending down to the lowest temperatures available. Diminishing activity was also found up to and above room temperature. Goldsmith (1956) reported that colemanite is also ferroelectric below -2.5°C. His measurements showed that the dielectric constant in the (010) direction rose from 20 at room temperature to about 7000 at the Curie point and dropped again to 18 well below this temperature. The half width of this peak was only 1° but it was typical of a second order transition. The spontaneous polarization is about $0.5 \mu C/cm^2$ and the coercive field about $10^4 V/cm$. Many of the hysterisis loops observed for different samples were quite asymmetric indicating some form of internal bias. Chynoweth (1957) using a very sensitive method of measuring pyroelectric activity, confirmed Davisson's measurements but emphasized that the more ideal specimens showed less activity on the high temperature side of the transition point. He concluded that colemanite is pyroelectric only below -6°C and is non-active and therefore centrosymmetric above this temperature. The tails at higher temperatures may be explained by internal space-charges giving an induced polarization in the centrosymmetric phase. These tails have also been observed in other ferroelectrics.

The point group was confirmed as being 2/m at room temperature and 2 below the transition, through the nuclear magnetic resonance studies of the boron sites by Holuj and Petch (1958, 1960). The splitting due to the interaction of the ^{11}B nuclear electric quadrupole moment and the electric field gradient tensor was followed continuously as the temperature was lowered and the transition found to be of second order. The changes observed to take place at the phase transition were small, which indicated, as Davisson had suspected, that the deviation from centro-symmetry in the ferroelectric state is small.

Little was known of the structure of any of the borate minerals until Christ, Clark and Evans (1954) solved the structure of colemanite using the Hauptman and Karle (1953) direct method of determining structure factor signs. This was a major advance both for the crystal chemistry of the hydrated borates and for the direct method which had been criticized by many x-ray diffractionists. The main structural unit of colemanite is a 6-membered ring of alternating boron and oxygen atoms. Two of the boron atoms are tetrahedrally coordinated and the other is triangularly coordinated. Each oxygen atom not shared by two borons has attached a hydrogen atom to form a hydroxyl group. The rings are polymerized into infinite chains through shared oxygen atoms between the rings. These chains of composition $(B_3O_4(OH)_3)_n^{-2n}$ which run parallel to the crystallographic a-axis are linked laterally through the Ca^{++} ions to form sheets perpendicular to the b-axis. The only bonds between sheets are the hydrogen bonds of the three hydroxyls and one water molecule per asymmetric unit. This sheet-structure accounts for the perfect cleavage obtainable on the (010) faces.

Hydrogen positions are not normally determined by x-ray techniques but they may be inferred from a consideration of interatomic distances. For hydrogen bonds between oxygen atoms, the inter-oxygen distance is commonly 2.6 to 2.8 Å. For the three hydroxyls in the asymmetric unit of colemanite, two hydrogen bonds were clearly indicated by the distances, but the third (O_5 to O_4, in Fig. 2, Chapter 2) was rather long (2.81 Å) and it was suggested that this bond is unstable with respect to two possible acceptor oxygen atoms. The single oxygen (O_9), which is not closely bonded to any boron atoms was assumed to be the water oxygen. Since it is situated at a distance of 2.76 Å from oxygen O_6, a normal hydrogen bond was inferred. Although O_9 is placed 2.70 Å from the water oxygen of the next unit cell and related to it by symmetry, the presence of the inversion centre mid-way between them requires a disordered bond system. If one hydrogen atom is placed in this bond full-time then the hydrogen atom of the other water molecule is forced into a non-centrosymmetric position. In order to satisfy symmetry requirements, Christ et al. proposed that one hydrogen of each water molecule enters into the water-water bond only half the time and at other times is involved in a bond to some other part of the structure, probably O_5.

That this disorder is dynamic rather than static is supported by proton resonance studies (Holuj and Petch, 1960) and infrared absorption studies (Blinc, Maracic and Pintar, 1960). The width of a proton resonance line caused by dipole-dipole interaction depends on the relative motion of the protons, being very narrow when rotation or translation is possible but broader when the motion of the protons is restricted by the structure. The transition to the ferroelectric state in colemanite is accompanied by a continuous broadening of this resonance line in the powdered samples used. This suggested a "freezing out" of the hydrogen disorder and was cited as a likely trigger for the transition to the polar state.

The point group of the low temperature phase of colemanite was clearly shown by Holuj and Petch to be 2 and since the direction of the spontaneous polarization is the b-axis the space group must be $P2_1$. X-ray evidence to support this was obtained when Perloff and Block (1960) obtained low temperature photographs of the $(h0\ell)$ reciprocal net showing weak spots for some reflections with odd values of the index h. The $(0k\ell)$ net photographs showed no change indicating the loss of only the glide plane in the transition.

The magnitude of the changes in the ^{11}B resonance signals indicated that, although the hydrogen atoms play an important role in the ferroelectric transition, there are also significant changes in the boron-oxygen framework. Some further indication of changes in the cation environment was found during a comprehensive study of the dielectric properties of colemanite by Wieder (1959, also Wieder, Clawson and Parkerson, 1962). While attempting to determine the exact temperature of the transition he noted a large discrepancy for samples from different sources. Chemical analyses of the samples showed a correlation between the transition temperature and impurity content; a higher Curie point being found for samples with small amounts of strontium impurity substituted for calcium, but a lower transition temperature if magnesium is the major impurity. Preliminary studies using "pure" synthetic colemanite showed a Curie point at -35°C and, more recently, Wieder, Clawson and Parkerson (1963) have synthesized the strontium isomorph of colemanite and proved it to be ferroelectric with a transition temperature of +30°C. Since the x-ray study places the water molecule and the long O_5-O_4 hydrogen bond adjacent to the cation position, they interpret these results in terms of the hydrostatic pressure of a larger ion in the region of unstable hydrogen bonds.

The proposals concerning the role of the hydrogen bonds in the ferroelectric behavior of colemanite cannot be resolved without an accurate knowledge of the hydrogen positions and the changes they undergo at the transition temperature. Since x-rays are scattered by electrons, the scattering from a hydrogen atom with one electron is almost completely lost in the presence of a strong scatterer such as calcium. For neutrons, however, the scattering is a nuclear process and the scattering power for almost all nuclides is of the same order of magnitude. In particular, the hydrogen scattering length is only slightly smaller in magnitude than those of oxygen, boron or calcium, the other constituents of colemanite. Actually the hydrogen scattering length is of the opposite sign to the others making hydrogen peaks more easily detectable on a fourier synthesis plot. Neutron diffraction has the further advantage over x-ray diffraction in that more accurate information is available at high scattering angles since the scattering does not fall off at high values of the Bragg angle. This allows more accurate refinement of the temperature parameters.

The main drawback for a neutron diffraction analysis is the relative weakness of monochromatic neutron sources (10^6 - 10^7 n/cm^2 - min as compared to x-ray generators with up to 10^{12} photons/sec of the characteristic radiation.) Although lower absorption factors for neutrons allow larger crystals and beams to be used, the detection apparatus is similarly larger and more complex. This disadvantage limits the use of neutron diffraction to certain special problems which cannot be done by x-ray methods.

Elucidating the atomistic mechanism of the ferroelectric transition in colemanite by determining the positions of the hydrogen atoms above and below the Curie point is certainly a worthy problem but even without this feature there is considerable interest in hydrogen bonds themselves as they occur in various structures. No hydrated borate material has been subjected to a neutron diffraction analysis until now, partly at least, because of the large absorption cross-section of boron for thermal neutrons and also because the scattering length of boron has not yet been determined. These additional features make the neutron diffraction of colemanite an especially worthwhile problem.

II. BASIC STRUCTURE OF COLEMANITE

A. Structure of the Hydrated Borates

Following the solution of the colemanite structure, a number of other hydrated borate minerals and synthetics have been solved by x-ray diffraction methods and several have been studied by nuclear magnetic resonance techniques. With the knowledge of the crystal chemistry of the borates which has been obtained from these studies, it has proved possible to derive a set of structural rules which are characteristic of all known hydrated borates. The following statement of the rules is from Christ (1960).

(1) Boron will link either three oxygen atoms to form a triangle or four to form a tetrahedron.

Boron is an electron-deficient element, that is, it has more stable orbitals than it has electrons. Only the two 2s electrons and the one 2p electron of neutral free boron are bonding electrons, but they may enter either sp^2 or sp^3 hybrid orbitals. The former arrangement leads to 3-fold planar triangular coordination and the latter to 4-fold tetrahedral bonding. The use of the fourth boron orbital leads to a net charge of -1 on an isolated tetrahedral group.

(2) Polynuclear anions are formed by corner sharing only of boron-oxygen triangles and tetrahedra in such a way that a compact insular group of low to medium charge results.

In general, the ratio of tetrahedral boron to total boron is equivalent to the ratio of the cation charge to total boron (Edwards and Ross, 1960), however, this postulate depends on the assumption that each oxygen will be shared by only two boron atoms. This has proved to be incorrect in the case of tunellite ($SrB_6O_9(OH)_2 \cdot 3H_2O$) (Clark, 1964) which has three triangles and three tetrahedra but the polyanion has a net charge of only -2. The phrase "corner sharing only" precludes the sharing of two oxygen atoms of one group with two of another but implies that a ring of three groups with only one common oxygen between each boron group may be quite stable. The stability of this ring is enhanced by the presence of one or two tetrahedra but the requirement of low to medium charge implies, as experience bears out, that three tetrahedra in one ring would be unstable.

(3) In the polyions of the hydrated borates, those oxygens not shared by two or more borons will always attach a proton and exist as hydroxyl groups.

The words "or more" were added by Clark (ibid) in order to include such structures as tunellite and perhaps others in which one oxygen atom is shared by three boron atoms.

(4) The insular groups may polymerize in various ways by splitting out water.

One example of this polymerization is the "conversion" of meyerhofferite to colemanite according to the equation:

$$n(B_3O_3(OH)_5)^{-2} = (B_3O_4(OH)_3)_n^{-2n} + nH_2O$$

In this process, discrete polyanions are joined to form an "infinite-chain" polyanion. The fusion of two rings is quite common but the first example of a three-ring polyanion is the tunellite structure.

On the basis of the above rules, Christ has predicted the most likely nature of the polyanions of a number of hydrated borates whose structures were unknown at that time. Recent structural and nmr studies have confirmed his predictions in all materials studied, with the exception of tunellite noted above. Some of the polyanions which have been found in mineral hydrated borates are shown schematically in Figure 1.

It is of interest to consider how the charge is distributed over the component atoms of the polyion. The single bond radius of boron, as determined from measurements of the boron-boron distance in various molecules, is given by Pauling (1960) as 0.81 Å. The corresponding value for oxygen is 0.74 Å. The sum of these for the expected boron-oxygen distance must be corrected for the partial ionic character of the bond which, according to the electronegativity difference is about 44%. Applying this correction gives 1.43 Å as the single-bond B-O distance. For trigonal coordination the fourth boron orbital gives greater stability through pi-bonds and, from the observed average B-O distance in various molecules of 1.37 Å, we may deduce about 20% of double-bond character for this coordination.

For tetrahedral bonds the observed B-O distance is 1.47 Å and this leads, in a similar way, to somewhat less than single-bond character. Using the formula of Pauling, the value of 0.86 for the bond number may be calculated.

Figure 1. Some examples of the polyanions found in typical hydrated borate minerals and synthetics.

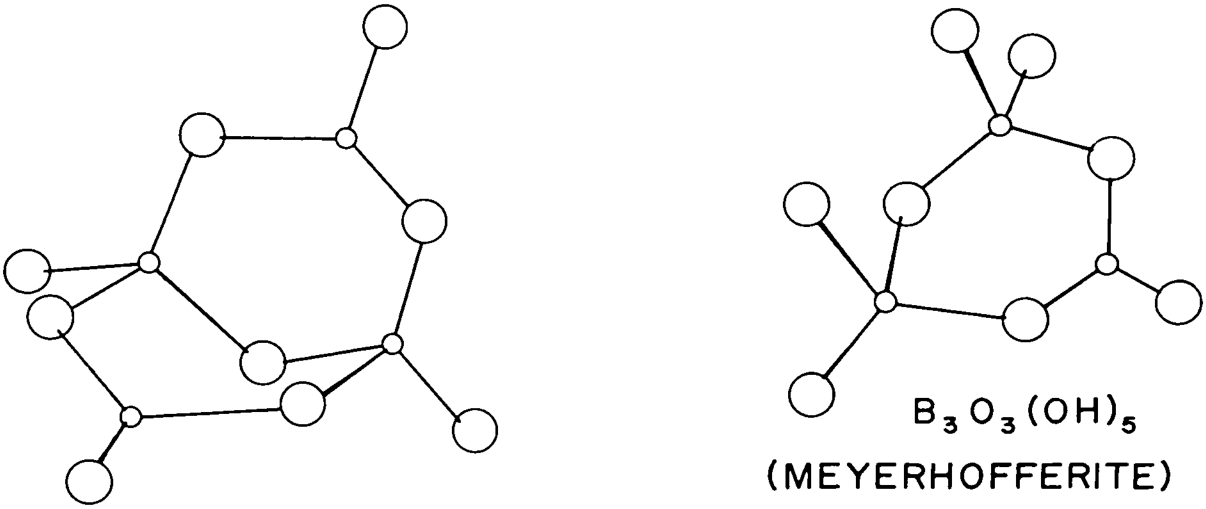

$B_4O_5(OH)_4$ (BORAX)

$B_3O_3(OH)_5$ (MEYERHOFFERITE)

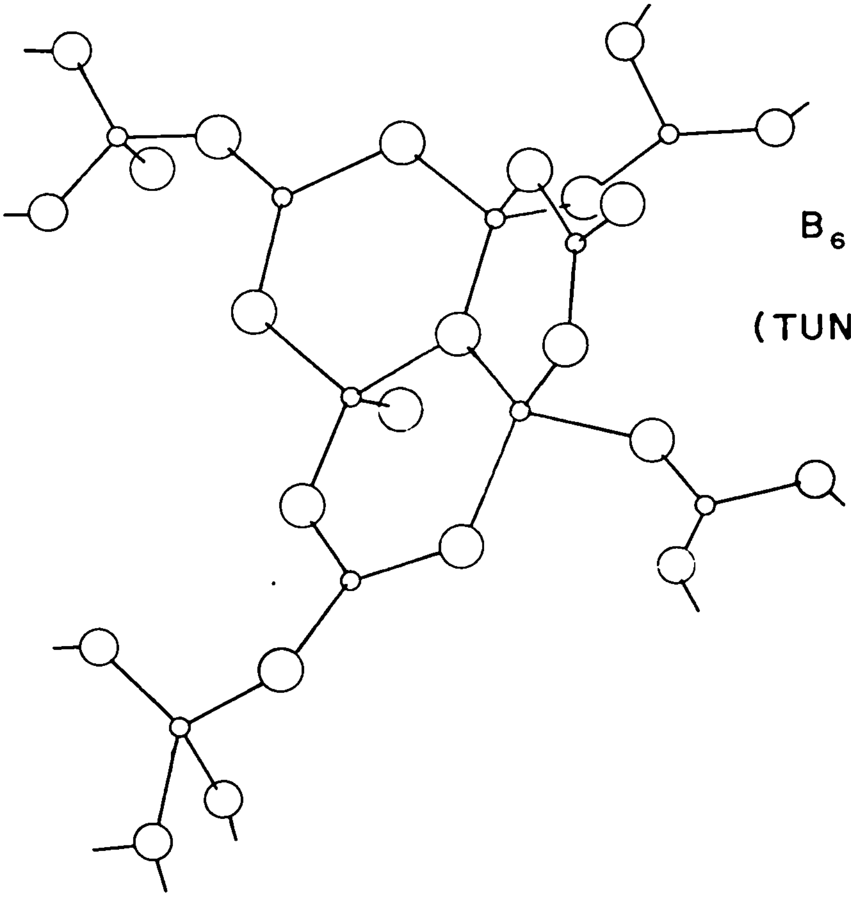

$B_6O_9(OH)_2$

(TUNELLITE)

FIGURE 1.

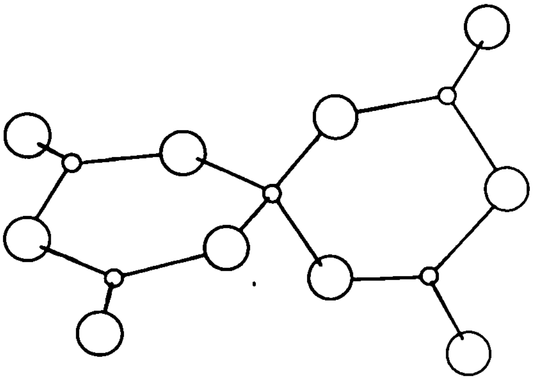

$B_5O_6(OH)_4$

(POTASSIUM PENTABORATE)

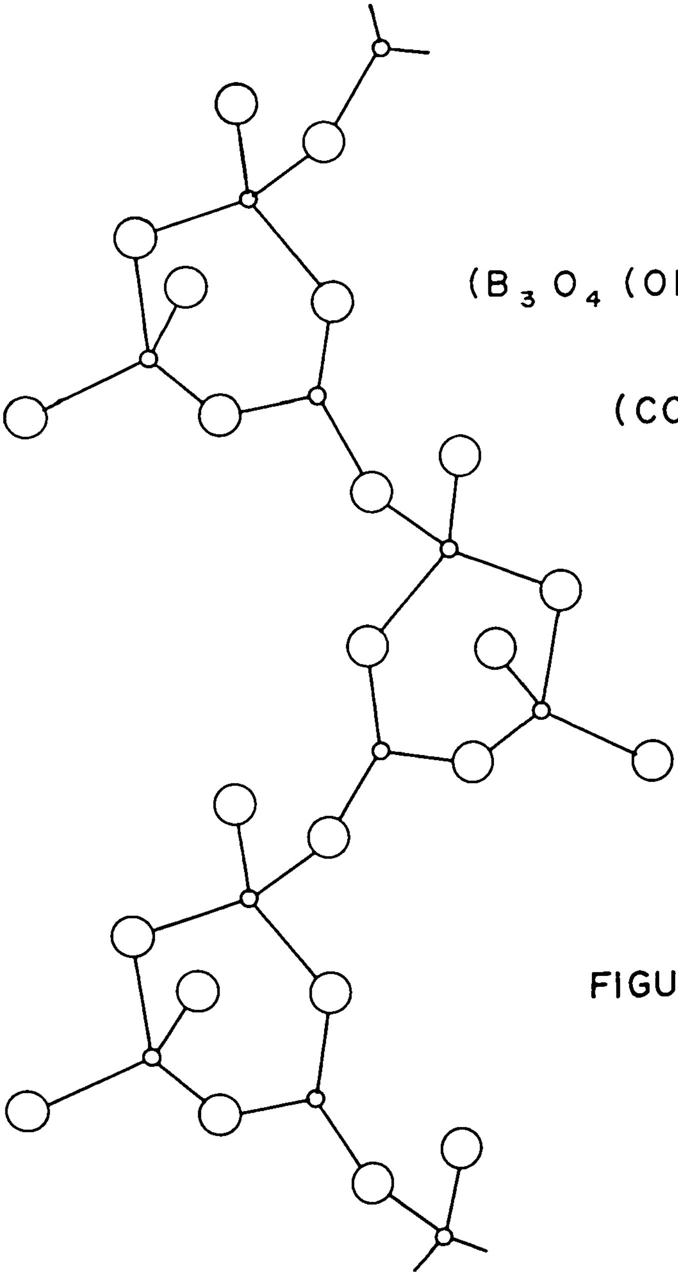

$(B_3O_4(OH)_3)$ - CHAIN

(COLEMANITE)

FIGURE 1 (CONT.)

According to these figures, the average charge distribution in a BO_3 triangle would be +0.72e on the boron and -0.24e on the oxygen (not considering the other bond of the oxygen atom). For tetrahedral boron, the distribution would be +1.32e on the boron and -0.58e on each oxygen atom.

B. Structure of Colemanite

The following crystallographic data were first described by Christ (1953):

Monoclinic; space group: $P2_1/a$- C_{2h}^5.

$a = 8.743 \pm 4$, $b = 11.264 \pm 2$, $c = 6.102 \pm 3$ A;

$\beta = 110^{\circ}\ 7' \pm 5'$

Cell contents: $4(CaB_3O_4(OH)_3 \cdot H_2O)$

Density: (calc.) = 2.419 g/cm^3, (obs.) = 2.42 g/cm^3

The main features of colemanite are shown in Figure 2* which is a projection on the (001) plane. The infinite chains of linked polyanions which run parallel to the a-axis (vertical) and the postulated

---

* The numbering system used here is taken from Clark et al. (1964) for the heavy atoms. Hydrogen atoms are labelled with two numbers, the first refers to the donor oxygen, the second to the acceptor or nominal acceptor in some cases. The system of primes used is the following: one prime denotes glide plane relationship at the high temperature; two primes denote screw axis relationship at both temperatures; and three primes indicate relation through the inversion centre. Atoms differing by two primes are then related by the screw axis in both space groups. Translation-equivalent atoms are not distinguished.

Figure 2. A projection of the structure of colemanite on the (001) plane as determined by Clark, Appleman and Christ (1964), including the postulated hydrogen bond system.

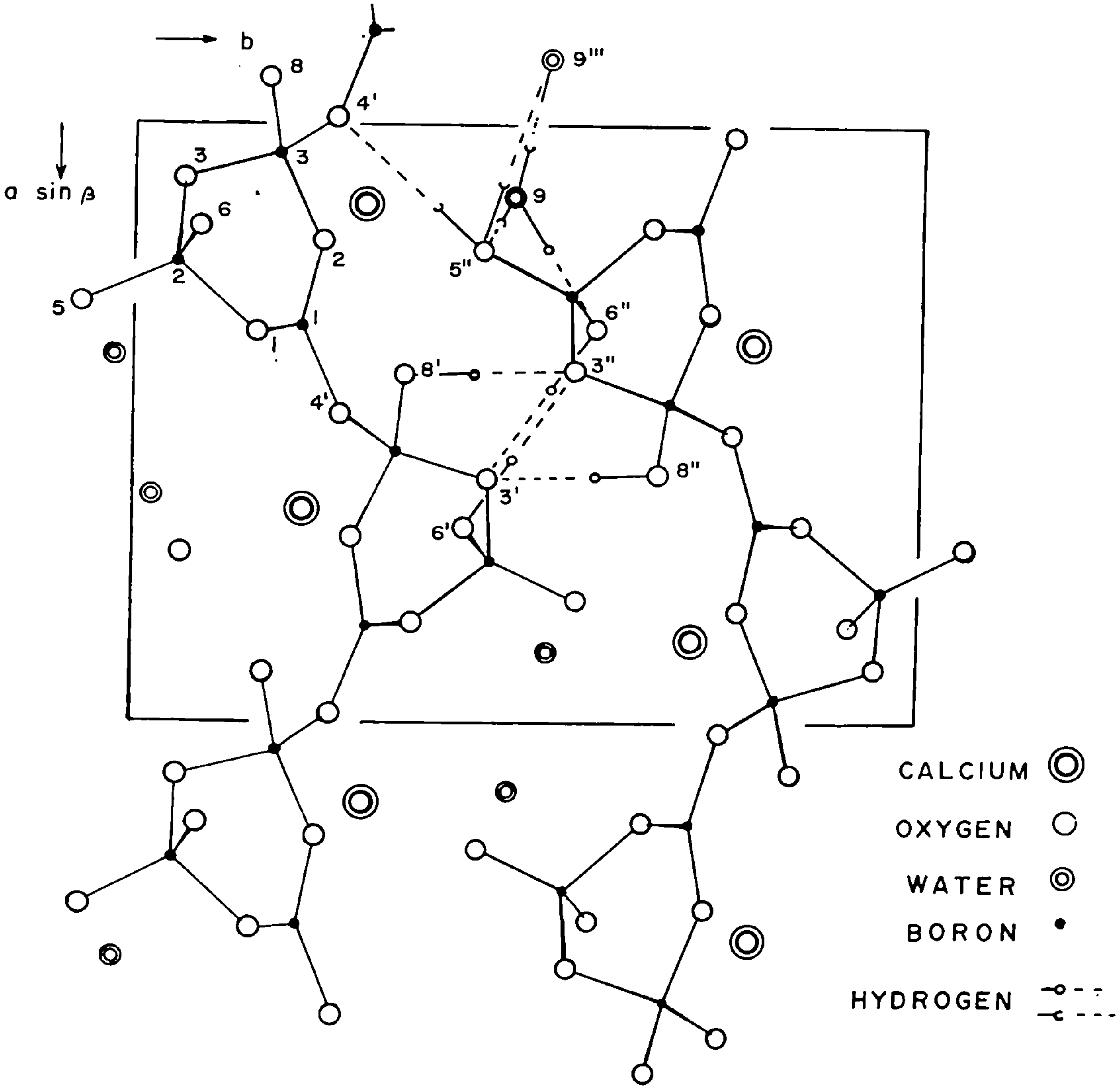
b
a sin β
8
4'
9'''
3
3
6
9
5''
2
2
5
1
6''
1
8'
3''
4'
8''
3'
6'
CALCIUM
OXYGEN
WATER
BORON
HYDROGEN

FIGURE 2.

hydrogen bonds which cross-link the chains in the b-direction are clearly shown. The individual and average bond lengths and angles in the boron triangle and two tetrahedra are listed in Table V, Chapter IV. These values agree closely with those found in many other structures, notably those in the series $Ca_2B_6O_{11}.xH_2O$ with x = 1, 5, 7, 9 and 13 studied by Clark, Appleman and Christ (1964). In this series colemanite has x = 5. The differences in the O-B-O angles from those expected for exact triangular or exact tetrahedral coordination are greater than the possible errors in these quantities and are thus significant. These strains allow a closer packing of the atoms in the polyanion and around the cation such that the resultant structure is more stable.

The oxygen atoms O_5, O_6 and O_8 are bonded to only one boron atom each and are identified as the three oxygen atoms belonging to the hydroxyl groups. Both O_6 and O_8 make close approaches to O_3''' with separations of 2.740 and 2.747 Å, respectively, and B-O-O angles of 117° and 113°, respectively. These values indicate that hydrogen bonds may be postulated unambiguously for these hydroxyls. Note that O_3 connects two boron tetrahedra and is the only oxygen in such a position in colemanite. It would likely have a slight excess of negative charge for this reason which will be reduced somewhat by the acceptance of two hydrogen bonds. In some others of the colemanite series, this oxygen does not take part in hydrogen bonding but this excess charge is balanced by the proximity of this atom to two calcium ions.

For the other hydroxyl oxygen, O_5, the most likely hydrogen linkage is not as clear. The O_5-O_4''' distance is 2.809 Å but the

B_2-O_5..O_4''' angle is 159°. Other possible acceptors for the O_5 hydrogen bond are O_9' and O_8' at distances of 2.94 and 2.93 Å, respectively. A bond with O_8' is unlikely since this would place the hydrogen atom too close to the calcium ion. This bond cannot therefore be postulated uniquely and it is quite possibly unstable to two or more alternatives.

O_9, the only oxygen atom not bonded to a boron atom, is the water oxygen. It is situated a distance of 2.769 Å from O_6'' and 2.708 Å from the related water oxygen O_9''' with O_9'''-O_9..O_6'' angle equal to 86° which allows a reasonably stable hydrogen bond system. The bond between O_9 and O_6'' is probably quite stable but the presence of the inversion centre between O_9 and O_9''' requires a disordered bond between the two. It was suggested that one hydrogen of each water molecule is placed in the O_9-O_9''' bond only half the time and each spends the rest of the time making a bond to O_5'' which is at a distance of 2.939 Å from O_9. By diffraction techniques, it cannot be decided whether the space average of the whole crystal or the time average of each bond is centrosymmetric but other studies show that the latter is the more likely case.

Calcium-oxygen distances are normally in the range of 2.3 to 2.9 Å with eight oxygen atoms surrounding the calcium ion. The calcium coordination observed for the various members of the colemanite series ranges from six bonds at an average distance of 2.42 Å, to eight bonds at an average distance of 2.48 Å. For colemanite there are seven oxygen atoms at distances between 2.42 and 2.56 Å and one at a distance of 2.89 Å. These are arranged in an irregular polyhedron with the average Ca-O separation equal to 2.45 Å for the nearest seven atoms.

III. DIFFRACTION MEASUREMENTS

A. The Diffractometer

The McMaster University pool-type research reactor first went critical in 1959 and shortly after this, a single-crystal neutron diffractometer, built by Petch, Brouwer, Torrie and Brown (1960), was operating in a semi-automatic manner. The study of natrolite (Torrie, Brown and Petch, 1964) proceeded while the apparatus was made fully automatic.

A plan view of the diffractometer is shown in Figure 3. The reactor is now operating continuously at a thermal power level of 2 megawatts, which gives a total neutron flux in the core of about 1.4×10^{13} n/cm^2-sec. A copper monochromator with its (111) planes set at an angle of 15° to the primary beam diffracts a secondary beam with a neutron energy of 0.068 ev (wavelength 1.087 Å) into the collimator. The flux in the monochromatic beam is about 10^5 n/cm^2-sec and its maximum useful cross-section is 2 cm square. After passing through the fission counter, used as a monitor, the beam impinges on the sample crystal and the undiffracted portion is eventually absorbed in the beam-stopper.

The diffractometer table is a General Electric x-ray spectrogoniometer adapted for neutron work. The crystal is mounted on a standard x-ray crystal mount which allows a particular crystallographic axis to be oriented so as to coincide with the axis of rotation of

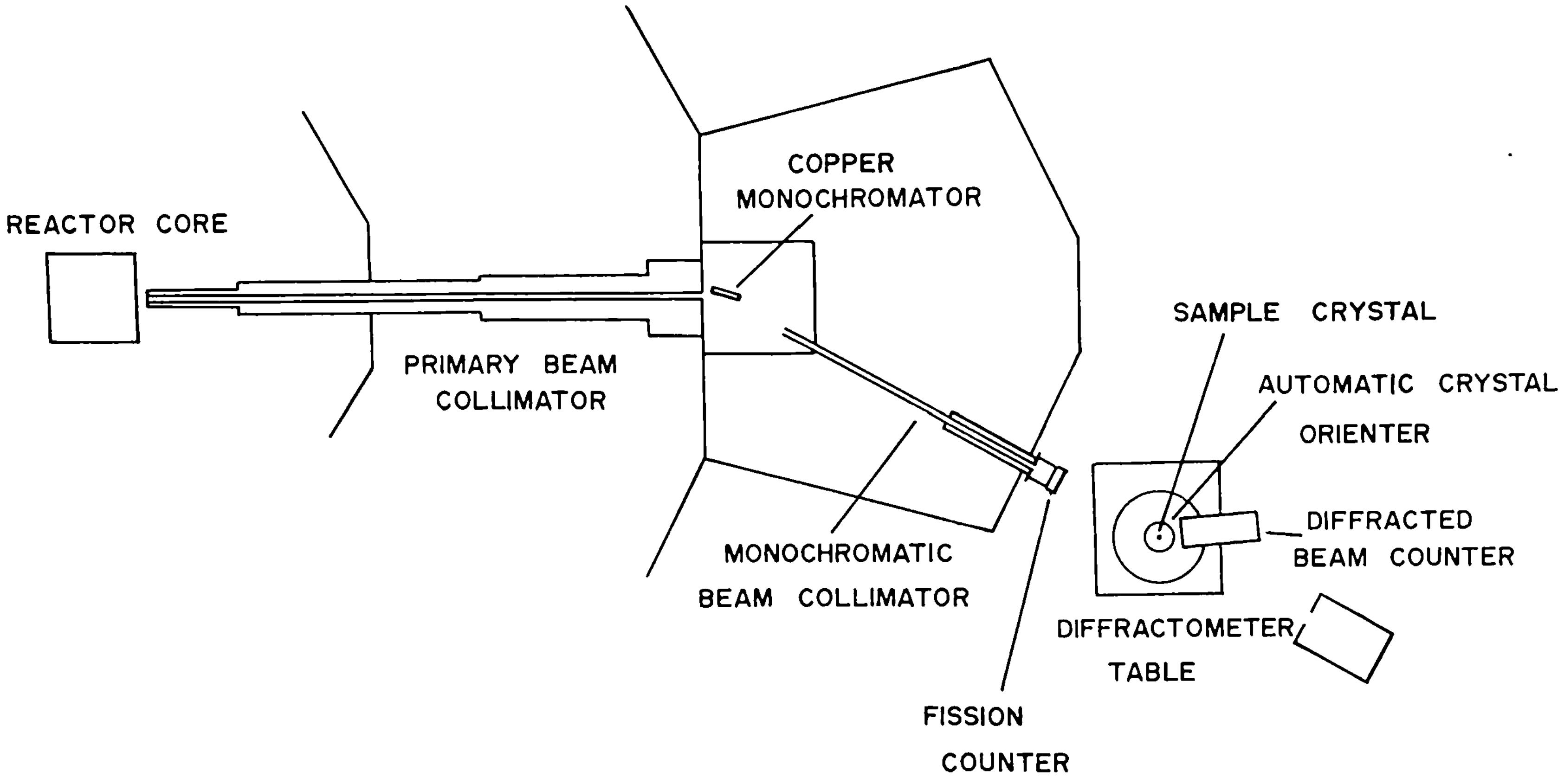

FIGURE 3. PLAN VIEW OF THE DIFFRACTOMETER AND BEAM PORT

the diffractometer. This mount then fits into place on the automatic crystal orienter which allows the operator to pre-select up to seventeen different orientations of the sample.

The diffracted beam from the crystal is measured by a BF_3 proportional counter mounted on the outer arm of the spectrogoniometer. This counter is coupled to rotate at twice the angular rate of the crystal support. During automatic operation, the counter is step-scanned with the direction of scan reversed for successive orientations of the sample. The details of the operation and the automation of this diffractometer have been described in full by Torrie (1963).

B. Low Temperature Device

To obtain information about colemanite in the ferroelectric state, the sample was cooled using a stream of cold, dry air from a liquid air storage vessel. A thermally insulated pipe conducted this stream from the storage vessel to a radiation shield covering the sample. A sufficient flow of air was ensured by dissipating a controlled amount of electrical power in a small resistor at the bottom of the storage vessel. The radiation shield consisted of two thin-walled aluminum tubes of diameter 1.0 and 1.4 cm arranged concentrically with insulating spacers. These fitted coaxially over the sample so as to isolate it thermally but not to interfere with its rotation between or during the scanning process. Condensation of water vapour from the room onto the outer tube was prevented by blowing a stream of air, heated if necessary, over the shield in the region of the crystal.

The temperature was measured by a thermocouple junction placed inside the shield just above the crystal. The emf developed by the thermocouple was recorded continuously by a chart recorder with a sensitivity of 100 mv full scale. This was calibrated by using the bulb of a mercury thermometer as a dummy crystal and noting the temperature and chart reading for various power levels dissipated in the storage vessel. About 20 watts were necessary to maintain a temperature of -20°C which required about 20 litres of liquid air over a 48 hour period.

During the collection of the entire set of low temperature measurements the crystal temperature was kept at -20°C ± 5°C. Temperature gradients down the length of the sample were estimated to be less than 1 C°/cm. Neutron scattering from the radiation shield increased the normal background level by less than 10%.

C. Colemanite Samples

The various sample crystals used in this analysis were all cut from the same single crystal specimen obtained from the Smithsonian Institute. This particularly clear example of colemanite was originally found in the Furnace Creek deposits of Death Valley, Inyo County, California. It had two large, almost perfectly transparent lobes which had grown out of a mass of slightly misaligned crystallites. Excellent growth faces allowed unambiguous determination of the crystallographic axes. Of the four sample crystals finally selected, two were cut from each lobe of the original specimen. All samples were shaped into cylinders with the axis of the cylinder coinciding with either the c or b crystallographic axes. The size and number of reflections measured with each crystal are listed in Table 1.

Data from crystal C-1 were taken for the purpose of making the extinction-absorption corrections to be described in the next

TABLE I. CRYSTAL SAMPLES USED IN THE NEUTRON DIFFRACTION OF COLEMANITE.

SAMPLE DESIGNATION	C-1	C-2	C-3	B-2
DIAMETER MM	1.160	2.025	2.818/ 2.785	2.414
HEIGHT MM	10.5	12.0	16.5	12.0
VERTICAL AXIS	C	C	C	B
NUMBER OF ROOM TEMPERATURE DATA	16	186	-	121
MAXIMUM BRAGG ANGLE DEGREES	45	60	-	72
NUMBER OF LOW TEMPERATURE DATA	-	50	139	172
MAXIMUM BRAGG ANGLE DEGREES	-	30	60	72

section. The majority of the room temperature (hk0) data was taken from crystal C-2. After 50 reflections had been measured at the lower temperature, slight cracks from excessive thermal cycling were noted and the remainder of the low temperature data was taken using crystal C-3. This crystal was slightly elliptical in cross-section and the major and minor axes are given in the Table. All the (h0ℓ) data, both at room temperature and at -20°C, were taken using crystal B-2. The low temperature data for both projections include all possible reflections out to a Bragg angle of 50°, beyond which point only the strong reflections were measured.

D. Corrections for Absorption and Secondary Extinction

The effect of nuclear absorption on the incident and diffracted beams is to reduce the observed intensity by a factor depending on the linear absorption coefficient, μ and the effective path length which is a function of the Bragg angle, θ. The intensity reduction due to extinction similarly depends on θ but also depends on the reflectivity, Q(hkℓ) which is proportional to the square of the structure factor, F(hkℓ) of the reflecting planes.

The ratio of the observed intensity, I_o, to that calculated for an ideally imperfect non-absorbing crystal of the same size, I_c, defines the absorption-extinction correction, E; $I_o = I_c \cdot E$ where $I_c = k \cdot Q \cdot V$, V is the volume of the crystal and k is a scaling factor. If μ and Q(hkℓ) are known, the ratio of I_o/I_c may be determined from a solution of the differential equations for the powers P_i and P_d in the incident and diffracted beams, respectively:

$$\frac{\partial P_d}{\partial x_d} = -(\mu+Q)P_d + QP_i$$

$$\frac{\partial P_i}{\partial x_i} = -(\mu+Q)P_i + QP_d \qquad (1)$$

where x_i and x_d are lengths measured in the directions of the incident and diffracted beams, respectively.

A computer program to integrate these equations with appropriate boundary conditions, written by Hamilton (1963), was obtained and adapted to run on the McMaster IBM 7040 computer. The representation of a crystal of arbitrary shape is accomplished in this program by reducing it to a number of right prismatic slices, each of which is defined by a set of horizontal lines forming the boundary of its cross-section. The area of each slice is then subdivided into an array of cells running along lines parallel to the directions of the incident and diffracted beams as shown in Figure 4. The boundary conditions are imposed by setting the value for the incident beam power equal to unity for all cells on the surface exposed to the incident beam, and setting the diffracted beam power equal to zero on the side away from that beam. Starting from the incident boundary and working towards the outgoing diffracted beam boundary, the contributions of each cell are accumulated and the sum of the outgoing beam contributions is compared to that which would have been obtained in the absence of extinction and absorption. This ratio, E, is divided into the observed intensity and the result, I_o/E should agree with the input value of I_c.

In this theory of extinction corrections, if μ is known, only one parameter is required to establish the relationship of I_o to Q. This is the constant of proportionality between Q and I_c, that is, the scaling factor, k.V. This factor may be most easily

FIGURE 4.

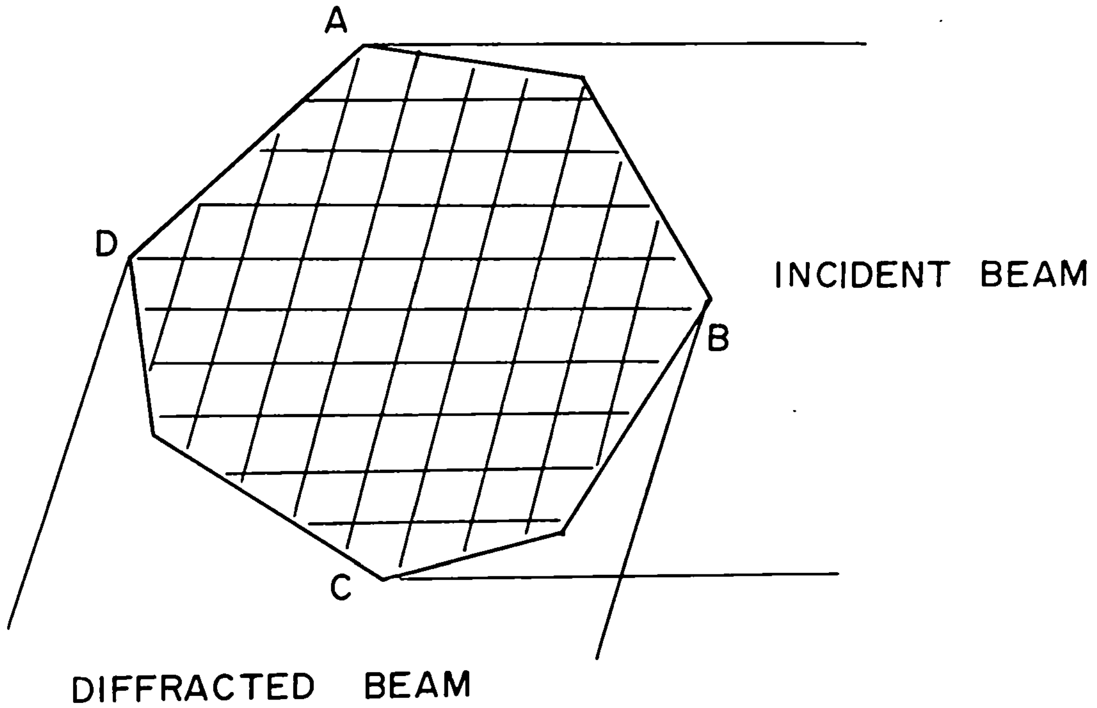

The cross-section of a crystal "slice" showing the array of cells used to calculate extinction-absorption correction. For cells on the boundary ABC the incident beam power is unity and for cells on the boundary DAB the diffracted beam power is zero. Only cells on the lower boundary DCB contribute to the "observed" diffracted beam. Up to 40,000 cells may be used in the actual calculation.

established from the measurement of a small number of reflections taken on two crystals of different diameters. From the definitions of E and I_c, we note that:

$$\frac{I_{o1}}{I_{o2}} = \frac{k.Q.V_1.E_1}{k.Q.V_2.E_2} = \frac{V_1}{V_2} \cdot \frac{E_1}{E_2} \qquad (2)$$

Since the quantity on the left can be measured and the volume ratio may be measured or calculated, the ratio of the correction factors for the two crystals is known. Using the computer program, a set of correction factors for representative values of Q and θ for each crystal may be obtained. If the ratios of the corresponding correction factors times the volume ratio are plotted as a function of Q, the resulting graph may be used to obtain for each observed intensity ratio a value of Q for that reflection. The data appropriate to crystals C-1 and C-2 are shown in Figure 5. Four typical values of the observed intensity ratio are also shown. With the values of Q thus determined for a number of reflections and the correction factors calculated, a graph of I_o/E against Q may be plotted. The slope of the best line through the points gives the reciprocal of the scaling factor, $(k.V)^{-1} = Q/I_c$. This information is shown in Figure 6 for crystal C-2.

Since Q/I_c is common to all data taken with the same crystal, only I_c need be determined for each new I_o to be corrected. A first approximation to I_o may be obtained by plotting I_c as a function of I_o, using the computer program to determine the correction factors for various values of Q and θ with the correct scale factor known. A set of curves appropriate to C-2 are shown in Figure 7. If the

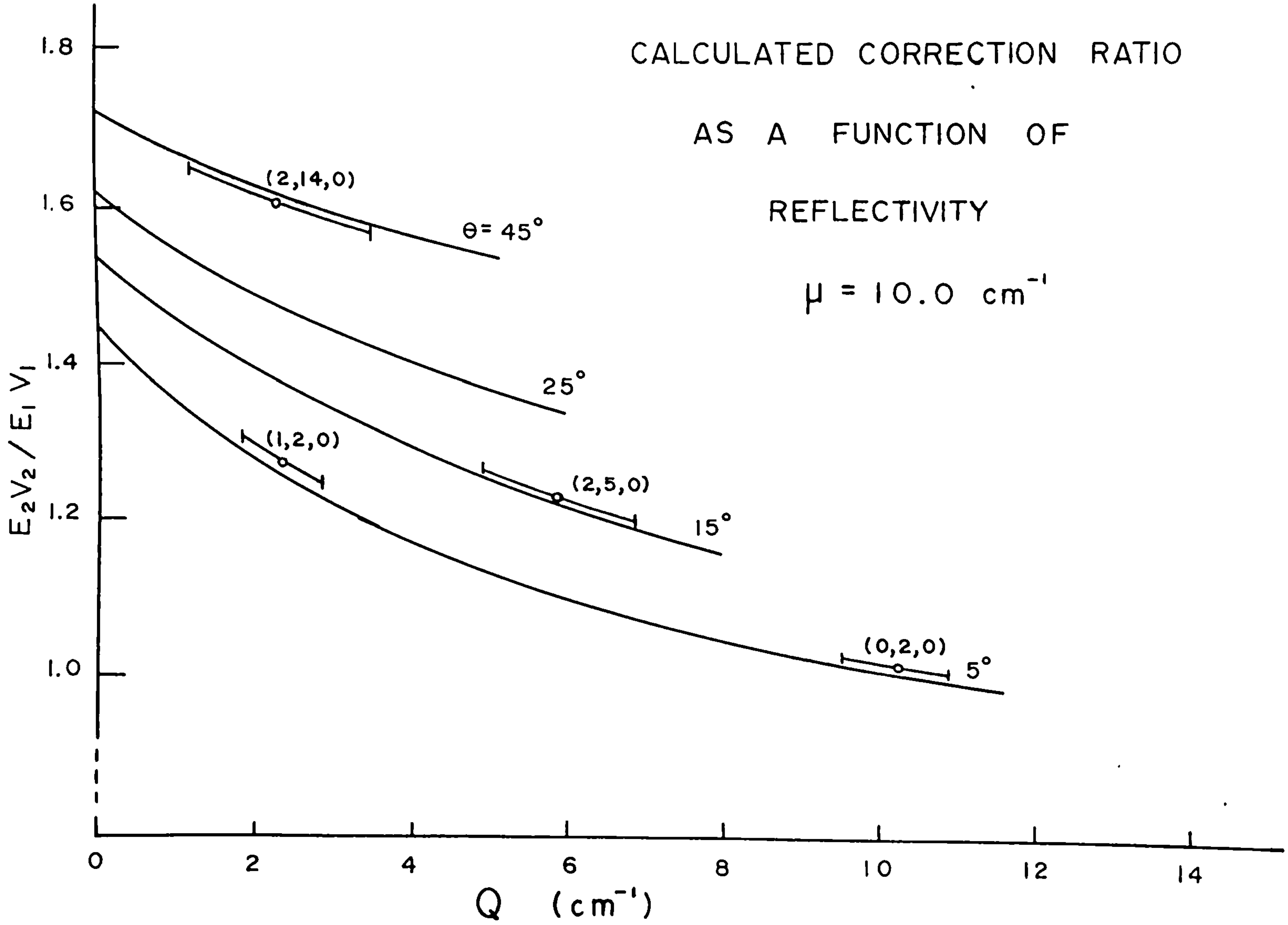
CALCULATED CORRECTION RATIO
AS A FUNCTION OF
REFLECTIVITY
$\mu = 10.0\ \text{cm}^{-1}$
E_2V_2 / E_1V_1
1.8
1.6
1.4
1.2
1.0
Q (cm⁻¹)
0
2
4
6
8
10
12
14
θ = 45°
25°
15°
5°
(2,14,0)
(1,2,0)
(2,5,0)
(0,2,0)

FIGURE 5.

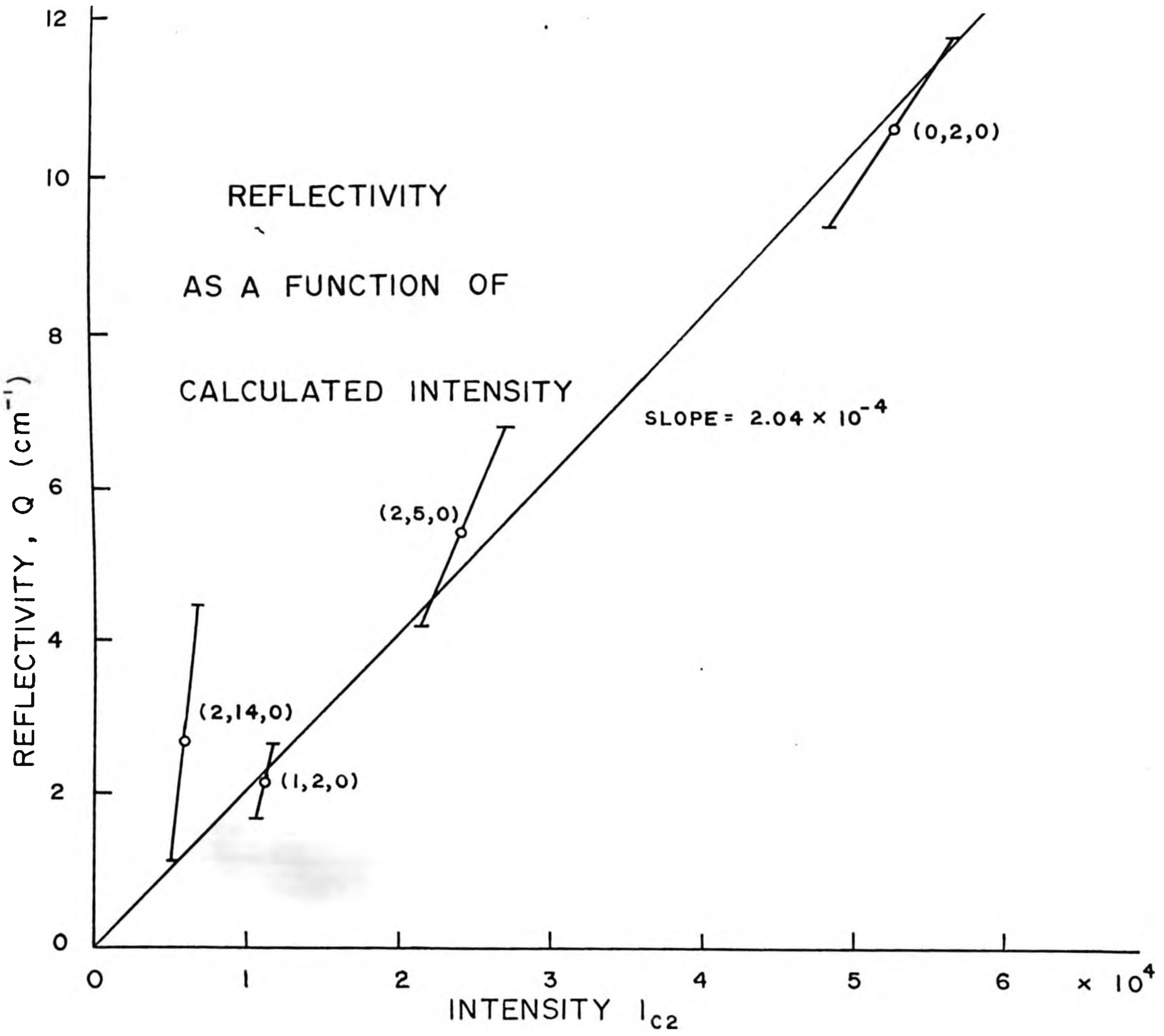
REFLECTIVITY
AS A FUNCTION OF
CALCULATED INTENSITY
SLOPE = 2.04 × 10^{-4}
(0,2,0)
(2,5,0)
(2,14,0)
(1,2,0)
REFLECTIVITY, Q (cm^{-1})
0
2
4
6
8
10
12
INTENSITY I_{c2}
0
1
2
3
4
5
6
× 10^4

FIGURE 6.

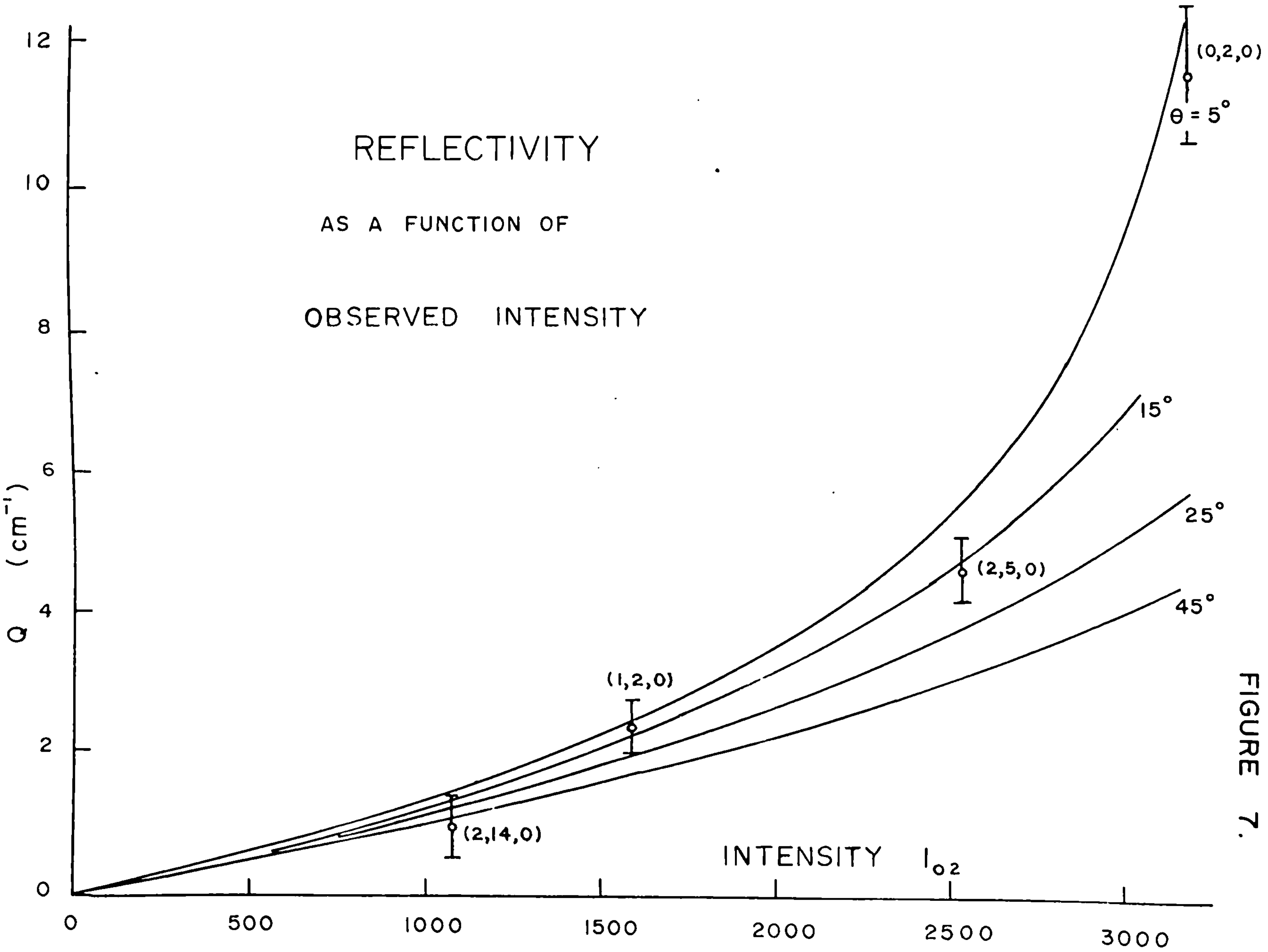
REFLECTIVITY
AS A FUNCTION OF
OBSERVED INTENSITY
Q (cm⁻¹)
0
2
4
6
8
10
12
INTENSITY I₀₂
0
500
1000
1500
2000
2500
3000
(0,2,0)
θ = 5°
15°
25°
45°
(2,5,0)
(1,2,0)
(2,14,0)

FIGURE 7.

first approximation is not sufficiently close, a process of iteration may be followed, using the calculated I_o/E as a better estimate of I_c.

A total of 16 reflections measured with C-1 and C-2 were used to obtain Q/I_c for this analysis. The uncorrected intensities, correction factors used and the final values of F_{obs} are given in Table II. The corrected data are in good agreement and further information on the adequacy of this method was obtained when 50 reflections taken at the lower temperature on C-2 and C-3 were compared; in nearly every case the agreement was within the possible error based on counting statistics alone.

The value of μ for true nuclear absorption may be calculated from the tabulated values of the atomic cross-sections, s_i, and the relative abundances, n_i, of the various nuclides present in the sample; $\mu = N_c \sum_i n_i s_i$, where N_c is the number of unit cells per unit volume and the sum is taken over all nuclides present in one unit cell.

The measured value, as determined by a good geometry transmission experiment will be larger, even in the absence of any Bragg reflection, due to incoherent neutron scattering. This effect is particularly noticeable for materials containing hydrogen. The effective value of the incoherent scattering cross-section of hydrogen depends on the relative binding energy of the proton with respect to the neutron energy, i.e., the effective mass of the proton in the structure (Bacon, 1962). For the protons in most materials a value for the incoherent scattering cross-section of about 30 barns is consistent with experimental data for neutron wave-lengths of about 1 Å. The experimental value of μ for colemanite is 10.0 ± 0.3 cm^{-1}

TABLE II. DATA TAKEN USING CRYSTALS C-1 AND C-2 TO OBTAIN EXTINCTION-ABSORPTION CORRECTIONS.

REFLECTION			OBSERVED INTENSITIES		CORRECTION FACTORS		CORRECTED STRUCTURE FACTORS		RATIO
H	K	L	I01	I02	E1	E2	F1	F2	F2/F1
0	2	0	3179	3229	0.15062	0.06162	63.66	100.34	1.58
1	2	0	1230	1567	0.30781	0.13980	30.47	51.26	1.68
2	0	0	568	821	0.34948	0.16742	20.66	35.87	1.73
2	2	0	751	1027	0.33961	0.16251	26.74	45.19	1.69
3	1	0	25	39	0.38337	0.19520	5.11	8.92	1.75
2	5	0	2055	2533	0.25975	0.11570	64.70	107.65	1.66
3	7	0	163	247	0.38251	0.20097	17.53	29.79	1.70
4	6	0	458	715	0.36645	0.18737	30.03	52.49	1.75
7	1	0	174	291	0.38645	0.20634	19.27	33.91	1.76
7	2	0	360	607	0.37658	0.19912	28.33	50.41	1.78
0	10	0	1382	1955	0.32161	0.16207	60.29	101.06	1.68
7	3	0	255	447	0.38360	0.20410	23.76	43.02	1.82
8	5	0	785	1249	0.36237	0.19518	45.28	77.83	1.72
2	14	0	666	1078	0.37834	0.21477	41.93	70.68	1.69
4	14	0	403	674	0.39477	0.22991	31.93	54.13	1.70
1	16	0	114	207	0.41327	0.24744	16.44	28.71	1.74

THE AVERAGE VALUE OF F2/F1 IS 1.715. THE SQUARE OF THIS NUMBER, 2.945, COMPARES FAVOURABLY WITH THE VOLUME RATIO, 2.95.

which coincides with the calculated value using an incoherent cross-section of 28 barns for the hydrogen atoms. The agreement was considered quite satisfactory and the experimental value was used in the correction of the room temperature data.

The values of Q/I_c and μ to be used in the correction of the low temperature data were first assumed to be the same as for the higher temperature data with Q/I_c divided by the volume ratio of the crystals used. When a reasonable sample of corrected structure factors had been obtained, a comparison with the corresponding room temperature values showed that the stronger reflections had been over-corrected, on the average, with respect to the medium and weak reflections. This indicated that a relaxation of the crystal at the lower temperature had reduced the degree of extinction by a significant amount. A value of Q/I_c about 10% lower was used to apply new corrections to the data and the refinement proceeded by the least squares adjustment method. It was immediately clear that the average atomic temperature factors were becoming smaller than could be reasonably expected from considerations of the ordering of the hydrogen bonds and the reduction in temperature. It was then suspected that the absorption coefficient had been underestimated. A value for μ of 10.5 cm^{-1} was tried and the refinement of the resulting structure factors brought the average of the temperature factors up to a value more consistent with the structural changes indicated.

Considering the effect of the structure on the effective proton mass and the changes in the hydrogen bonds at the lower temperature, an increase in the effective absorption coefficient is to be expected. The value of 10.5 cm^{-1} corresponds to an average incoherent cross-section for the hydrogen atoms of 35 barns.

E. Refinement of Data

When the room temperature (hk0) measurements had been completed, the data were first corrected for absorption only, using the correction factors tabulated in the International Tables for X-ray Crystallography, Vol. II. First approximations to the positions of the hydrogen atoms were obtained from the x-ray structural refinement, (Christ, Clark and Evans, 1958) by assuming linear O-H-O bonds and O-H distances of 1 Å between each hydrogen atom and its donor oxygen atom. Using the positional parameters for the heavy atoms given by Christ et al., structure factors were calculated including, and also omitting, the contributions of the hydrogen atoms. Fourier syntheses of the differences between the observed and the calculated partial structure factors were obtained in an effort to improve the parameters of the hydrogen atoms. The signs of the observed structure factors were taken as those of the calculated total structure factors. A value of 0.40 (in units of 10^{-12} cm.) was used as a first guess at the magnitude of the scattering length of boron. This was soon shown to be too low and the value was increased in steps to 0.49 which was used until further refined by the least squares program. It became clear that the stronger reflections had suffered considerable reduction due to secondary extinction and would have to be corrected before the refinement could continue. The best value of the agreement factor, R, obtained up to this point was 0.24.

Once the extinction corrections were made, using the methods described in the previous section, the agreement factor was reduced to about 0.12 quite quickly using difference syntheses. By this time, the least squares refinement* program (Busing, Martin and Levy, 1962) had been adapted to run on the IBM 7040 computer and only a few cycles of refinement were needed to reduce the residual to 0.06. Up to this point, isotropic temperature factors had been used for each atom. When these were converted to anisotropic form, further refinement was possible and the value of the residual was reduced to 0.029. During this stage of the refinement the positional parameters of the heavy atoms were also allowed to vary but they changed very little from the values given by Christ et al.

In the process of least squares refinement, the thermal parameters for hydrogen H_{99} of the water molecule and H_{54} of hydroxyl O_5, became markedly anisotropic, suggesting that these hydrogen atoms might be alternating between two distinct positions rather than simply vibrating with large amplitudes. To test this hypothesis, H_{99} and H_{54} were each replaced by two atoms with half the normal scattering length. These were placed in positions inferred from the magnitude and orientation of the major axis of the temperature factor ellipses of the original atoms. Isotropic thermal parameters were assigned to all atoms in this model as it was felt that

---

* A brief description of the mathematical basis of the least squares method of refinement is given in Appendix 1. This method makes use of the weighted residual, defined by:

$$R = \left\{\sum w(F_o - F_c)^2\right\}^{1/2} \Big/ \left\{\sum wF_o^2\right\}^{1/2}$$

This is the agreement factor quoted in the remainder of this section.

anisotropic temperature factors for the "half atoms" would defeat the purpose of the test. When the least squares program had been revised to permit the mixing of isotropic and anisotropic thermal parameters during refinement, the latter were assigned to all atoms except the "half atoms" which were given isotropic temperature factors. The agreement factor for the final set of room temperature parameters was 0.020.

For the analysis of the low temperature data, initial parameters were obtained from the room temperature values by displacing each atom very slightly in such a way that the glide plane relationship was destroyed. The least squares refinement process converged rapidly in spite of the fact that the original displacements were arbitrary and in many cases in the wrong direction. Due to the limited amount of data, only isotropic temperature factors could be used. However, since much of the anisotropic motion of the hydrogen atoms is "frozen out" below the Curie point, isotropic temperature factors proved to be quite adequate. When the data taken on crystal C-3 had been partially refined, the data from C-2 were corrected for absorption and extinction. These data had not been previously used because of the cracks which had appeared in the sample crystal. However, after the correct relative scale had been established, it was clear that the agreement between the two sets of data was within experimental error and weighted averages of the scaled values were used in the remainder of the refinement. The agreement factor obtained using the final set of parameters for this projection was 0.018.

Refinement of the (h0l) room temperature data started when 60 reflections were available. Initial values for the z-coordinates of the heavy atoms were taken from Clark, Appleman and Christ (1964). For the hydrogen atoms it was assumed that each of H_{63}, H_{83} and H_{96} were involved in linear bonds and that the donor oxygen-hydrogen distance was equal to 1 Å. Coupled with the x-coordinates previously obtained, this assumption allowed the calculation of z-parameters which proved to be quite good approximations. For hydrogens H_{54} and H_{99}, however, the only assumption which could be made was that the O-H distance would probably be 1 Å. Using the x-coordinates obtained previously, this still left two alternatives for each "half-atom". A consideration of the calculated bond angles for these positions showed that two of the eight alternatives were unlikely. Calculation of the structure factors using various pairs of the remaining possibilities soon gave the correct combination and the refinement proceeded using the method of least squares.

Further data were added in groups of about 20 reflections as they became available until all reflections out to the limit of the apparatus had been measured, a total of 121. Anisotropic temperature factors were then introduced and refined. However, there are several pairs of atoms whose positions, projected on the (010) plane are nearly identical and some of the temperature factors became quite unrealistic because of the large interaction of the parameters for these atoms. It was therefore decided to retain isotropic temperature factors and, further, to vary only one of each pair of the interacting parameters during any one cycle of refinement. In this manner, the parameter adjustment proceeded until no further reduction of the residual below 0.06 could be obtained. The temperature parameters had then stabilized but on comparison with those of the (hk0) refinement, showed that the latter were all higher by approximately the same additive constant.

The reason for this difference is not clear but it is not surprising that, for crystals with rather high absorption coefficients, such systematic inconsistencies should appear. The form of the functional dependence on the Bragg angle of the correction factors for pure absorption and for thermal motion are sufficiently similar that a systematic error in the absorption correction would appear as a constant additive error in the temperature factors. This will not be reflected in the value of the residual obtained nor should there be any significant effect on the positional parameters.

In order to make the (h0ℓ) data consistent with the (hk0) data, which were believed to be the more accurately corrected of the two sets, the average difference, δB, in the refined temperature factors was found and the factor, $\exp(-\delta B \sin^2\theta/\lambda^2)$ was multiplied into the (h0ℓ) data. The refinement of all three positional parameters and isotropic temperature factors of all atoms then proceeded using both sets of data. The parameters obtained at the end of this stage of the refinement are considered those most representative of the total room temperature structure of colemanite and are quoted along with their standard errors in the next section. The agreement factor for this set of parameters is 0.049.

The final stage of refinement of the data taken at -20°C proceeded in a similar manner as for the room temperature data. First, the refinement of the parameters using the (h0ℓ) data was taken as far as possible and the average difference between temperature factors obtained from the (hk0) and (h0ℓ) data was found. This value of δB was approximately the same as for the room temperature data δB = 0.20 and was used in the same way to make the two sets of data consistent. Finally, the parameters of all the atoms were simultaneously adjusted by least squares methods until no further reduction of the residual could be obtained. The final set of parameters for this structural phase gave an agreement factor of 0.038.

IV. RESULTS AND DISCUSSION

A. Numerical Results

The final room temperature parameters are given in Table III along with the results of the x-ray refinement by Clark et al. (1964). The agreement is generally good, there being only 6 of the 36 positional parameters which differ by more than the sum of the assigned errors for the two sets. In general, the largest discrepancies are in the z-coordinates which, in this structure, are much more difficult to obtain accurately by projection data alone because of the overlap of atomic positions in the (010) projection. This overlapping is a possible cause of some of these differences, although the z-coordinate of the water oxygen, which is not overlapped in this projection, shows a large and possibly significant difference.

The average accuracy of the positions of the hydrogen atoms is about 0.015 Å for the three normal hydrogens and 0.03 to 0.08 Å for the "half-time" hydrogen atoms. The average accuracies for the positions of the boron, oxygen or calcium atoms is 0.007 Å.

The temperature factors as refined by neutron diffraction show fair correspondence to those of the x-ray work for the calcium atoms and the oxygen atoms but the boron temperature factors are consistently lower. The latter differences may reflect an error in the value of the boron scattering length, although it is possible that both sets of values are accurate, since neutrons and x-rays

TABLE III. POSITIONAL AND THERMAL (B) PARAMETERS FOR THE ROOM TEMPERATURE STRUCTURE OF COLEMANITE. ERRORS QUOTED REFER TO THE LAST GIVEN FIGURE.

		NEUTRON DIFFRACTION THIS REFINEMENT		X-RAY DIFFRACTION CLARK ET AL. 1964.	
		PARAMETER	ERROR	PARAMETER	ERROR
CALCIUM	X	0.1347	± 8	0.1348	± 2
	Y	0.2886	6	0.2891	1
	Z	0.7340	17	0.7368	2
	B	1.15	9	0.80	2
BORON 1	X	0.3344	6	0.3342	8
	Y	0.2118	5	0.2129	7
	Z	0.3104	11	0.3135	11
	B	0.38	7	0.78	7
BORON 2	X	0.2211	6	0.2210	8
	Y	0.0523	4	0.0521	6
	Z	0.4949	23	0.4964	11
	B	0.32	7	0.68	7
BORON 3	X	0.0401	5	0.0400	8
	Y	0.1711	5	0.1711	6
	Z	0.1654	11	0.1633	11
	B	0.39	7	0.67	7
OXYGEN 1	X	0.3424	6	0.3421	6
	Y	0.1495	5	0.1478	4
	Z	0.5081	12	0.5099	8
	B	0.84	9	0.99	6
OXYGEN 2	X	0.1889	5	0.1886	6
	Y	0.2311	4	0.2313	4
	Z	0.1413	10	0.1383	8
	B	0.48	6	0.74	5
OXYGEN 3	X	0.0877	5	0.0872	5
	Y	0.0555	5	0.0558	4
	Z	0.2700	10	0.2713	8
	B	0.44	6	0.69	5
OXYGEN 4	X	0.4807	5	0.4814	6
	Y	0.2529	5	0.2531	4
	Z	0.3140	11	0.3148	8
	B	0.63	6	0.88	6
OXYGEN 5	X	0.2962	7	0.2964	7
	Y	-0.0670	7	-0.0664	5
	Z	0.5154	27	0.5146	9
	B	1.09	9	1.26	7

TABLE III. (CONTINUED)

		PARAMETER	ERROR	PARAMETER	ERROR
OXYGEN 6	X	0.1672	± 7	0.1669	± 6
	Y	0.0775	5	0.0771	5
	Z	0.6925	12	0.6971	9
	B	0.84	7	1.07	6
OXYGEN 8	X	-0.0801	6	-0.0793	6
	Y	0.1633	5	0.1638	4
	Z	-0.0725	13	-0.0720	8
	B	0.73	7	0.85	6
OXYGEN 9	X	0.1137	7	0.1135	7
	Y	0.4823	6	0.4818	6
	Z	0.9040	15	0.8985	11
	B	1.53	10	1.54	8
HYDROGEN 63	X	0.0772	15		
	Y	0.0250	12		
	Z	0.6968	26		
	B	1.93	19		
HYDROGEN 83	X	-0.0793	11		
	Y	0.0833	8		
	Z	-0.1274	26		
	B	1.47	14		
HYDROGEN 96	X	0.2012	15		
	Y	0.5200	15		
	Z	0.0244	32		
	B	3.40	27		
HYDROGEN 54C	X	0.3824	35		
	Y	-0.0830	31		
	Z	0.6529	69		
	B	3.51	57		
HYDROGEN 54D	X	0.3123	26		
	Y	-0.0988	30		
	Z	0.6782	49		
	B	1.91	36		
HYDROGEN 99A	X	0.0267	63		
	Y	0.5055	101		
	Z	0.9356	102		
	B	6.06	114		
HYDROGEN 99B	X	0.0745	55		
	Y	0.5182	52		
	Z	0.7089	91		
	B	4.28	75		

are scattered by different processes and hence actually measure different quantities, (Bacon, 1962A, Hamilton, 1962).

The parameters obtained from the refinement of the data taken at -20°C are shown in Table IV. Since the number of parameters is twice as large for the non-centrosymmetric low temperature structure, the accuracy is less than for the centric structure. Although the number of ($h0\ell$) reflections theoretically observable is doubled for the low temperature space group, the low precision with which those reflections with odd values of the index h could be measured severely limited their contribution to the accuracy of the refinement. The average accuracy of the positional coordinates is 0.02 to 0.04 Å, being somewhat better for the x-coordinates which are determined by both the ($h0\ell$) and ($hk0$) sets of data. The accuracy of the hydrogen parameters is comparable to the other atoms for this refinement.

Although the individual temperature factors differ greatly between the two refinements, a comparison of the average for each psuedo-related pair with the temperature parameter of the equivalent atom at room temperature shows a definite correspondence. Because of the large errors in these quantities, it is not likely that the differences between the temperature factors of the psuedo-related atoms are as large as indicated, although some differences are to be expected. The average of the two, however, is probably a good measure of any changes from the room temperature values. The arithmetic mean of the temperature factors of all the atoms is lower by 10% for the low temperature refinement. This is approximately the change expected from the relative change in temperature (40° in 300 K°). There is, however, a significant reduction in the individual tempera-

TABLE IV. POSITIONAL AND THERMAL (B) PARAMETERS FOR THE LOW TEMPERATURE STRUCTURE OF COLEMANITE. THE CHANGE IN EACH PARAMETER FROM THE CORRESPONDING ROOM TEMPERATURE VALUE IS ALSO INDICATED. ERRORS AND CHANGES REFER TO THE LAST FIGURES QUOTED.

		UNPRIMED UNIT			PRIMED UNIT		
		PARAMETER	ERROR	CHANGE	PARAMETER	ERROR	CHANGE
CALCIUM	X	0.3918	± 25	+71	0.8795	± 24	-52
	Y	0.2864	20	-22	0.2095	19	-19
	Z	0.7301	48	-39	0.7447	44	+107
INDIVIDUAL	B	1.11	+0.39		1.00	+0.36	
AVERAGE	B	1.06	ROOM TEMPERATURE B			1.13	
BORON 1	X	0.5817	20	-27	0.0883	21	+59
	Y	0.2151	30	+51	0.2895	32	+31
	Z	0.3030	67	-74	0.3054	36	-70
INDIVIDUAL	B	0.38	0.26		0.27	0.21	
AVERAGE	B	0.33	ROOM TEMPERATURE B			0.38	
BORON 2	X	0.4718	17	+7	0.9709	19	-2
	Y	0.0602	28	+97	0.4583	29	-94
	Z	0.4922	62	-27	0.4887	77	-62
INDIVIDUAL	B	0.09	0.31		0.34	0.36	
AVERAGE	B	0.22	ROOM TEMPERATURE B			0.32	
BORON 3	X	0.2946	19	+45	0.7863	19	-38
	Y	0.1760	30	+49	0.3340	27	+51
	Z	0.1668	46	+14	0.1611	40	-48
INDIVIDUAL	B	0.45	0.30		0.28	0.26	
AVERAGE	B	0.37	ROOM TEMPERATURE B			0.39	
OXYGEN 1	X	0.5961	19	+37	0.0876	18	-48
	Y	0.1470	30	-7	0.3477	27	-28
	Z	0.5085	45	+4	0.5046	42	-35
INDIVIDUAL	B	1.06	0.30		0.49	0.25	
AVERAGE	B	0.78	ROOM TEMPERATURE B			0.84	

TABLE IV. (CONTINUED)

		UNPRIMED UNIT			PRIMED UNIT		
		PARAMETER	ERROR	CHANGE	PARAMETER	ERROR	CHANGE
OXYGEN 2	X	0.4422	± 18	+33	0.9348	± 19	-41
	Y	0.2278	34	-35	0.2671	36	-18
	Z	0.1371	32	-42	0.1456	37	+43
INDIVIDUAL	B	0.28	0.24		0.73	0.28	
AVERAGE	B	0.50		ROOM TEMPERATURE B		0.48	
OXYGEN 3	X	0.3317	21	-60	0.8399	17	+22
	Y	0.0563	32	+8	0.4480	31	+35
	Z	0.2699	46	-1	0.2676	21	-24
INDIVIDUAL	B	0.92	0.32		0.26	0.25	
AVERAGE	B	0.59		ROOM TEMPERATURE B		0.44	
OXYGEN 4	X	0.7298	21	-9	0.2318	22	+11
	Y	0.2547	32	+18	0.2498	34	+27
	Z	0.3149	44	+9	0.3150	44	+10
INDIVIDUAL	B	0.66	0.31		0.78	0.34	
AVERAGE	B	0.72		ROOM TEMPERATURE B		0.63	
OXYGEN 5	X	0.5476	26	+14	0.0447	21	-15
	Y	-0.0623	36	+47	0.5711	32	+41
	Z	0.5189	79	+35	0.5078	73	-76
INDIVIDUAL	B	1.76	0.44		0.71	0.34	
AVERAGE	B	1.24		ROOM TEMPERATURE B		1.09	
OXYGEN 6	X	0.4123	21	-49	0.9239	22	+67
	Y	0.0772	34	-3	0.4227	32	+2
	Z	0.6748	41	-177	0.6983	46	+58
INDIVIDUAL	B	1.17	0.25		0.93	0.32	
AVERAGE	B	1.05		ROOM TEMPERATURE B		0.84	
OXYGEN 8	X	0.1715	22	-84	0.6701	17	-98
	Y	0.1588	36	-45	0.3337	31	-30
	Z	-0.0685	48	+40	-0.0785	35	-60
INDIVIDUAL	B	1.48	0.37		0.38	0.25	
AVERAGE	B	0.92		ROOM TEMPERATURE B		0.73	

TABLE IV. (CONTINUED)

		UNPRIMED UNIT			PRIMED UNIT		
		PARAMETER	ERROR	CHANGE	PARAMETER	ERROR	CHANGE
OXYGEN 9	X	0.3605	± 20	-32	0.8681	± 28	+44
	Y	0.4867	27	+44	0.0255	32	+78
	Z	0.8992	38	-48	0.9095	54	+45
INDIVIDUAL	B	0.77	0.25		2.35	0.47	
AVERAGE	B	1.56	ROOM TEMPERATURE B			1.53	
HYDROGEN 63	X	0.3312	38	+40	0.8217	31	-55
	Y	0.0189	37	-61	0.4676	39	-74
	Z	0.6866	74	-102	0.6999	59	+31
INDIVIDUAL	B	1.73	0.56		1.18	0.44	
AVERAGE	B	1.46	ROOM TEMPERATURE B			1.93	
HYDROGEN 83	X	0.1619	30	-88	0.6815	29	+108
	Y	0.0840	36	+7	0.4146	35	-21
	Z	-0.1351	65	-77	-0.1192	82	+82
INDIVIDUAL	B	1.10	0.46		1.16	0.50	
AVERAGE	B	1.13	ROOM TEMPERATURE B			1.47	
HYDROGEN 96	X	0.4537	56	+25	0.9560	35	+48
	Y	0.5135	75	-65	-0.0200	50	0
	Z	0.0159	112	-85	0.0413	72	+169
INDIVIDUAL	B	4.55	0.95		1.89	0.55	
AVERAGE	B	3.22	ROOM TEMPERATURE B			3.40	
HYDROGEN 54	X	0.5645	23	+22	0.1319	29	-5
	Y	-0.0929	36	+23	0.5772	38	-58
	Z	0.6818	43	-36	0.6542	60	+13
INDIVIDUAL	B	1.51	0.33		2.76	0.52	
AVERAGE	B	2.14	ROOM TEMPERATURE B			2.71	
HYDROGEN 99	X	0.3300	36	+55	0.7631	62	-136
	Y	0.5232	37	+49	0.0057	76	+2
	Z	0.7276	85	+187	0.9333	93	-23
INDIVIDUAL	B	2.48	0.53		4.86	0.71	
AVERAGE	B	3.84	ROOM TEMPERATURE B			5.17	

ture factors for all the hydrogen atoms relative to those of the heavier atoms.

The most striking differences between the two structures are the changes observed for hydrogen atoms, H_{99} and H_{54}. One of the two "part-time" positions for each of these at higher temperature is completely vacant at the lower temperature while for the other, the scattering density indicates full-time occupation. These changes can be most easily seen by comparison of Figures 8 and 9 with 10 and 11. These are Fourier syntheses of hydrogen scattering only, projected on the (001) and (010) planes at room temperature and the same two projections, respectively, at -20°C.

For the other atoms, the changes in positional parameters are generally small and in many cases may not represent significant structural changes. The shifts indicated for the boron atoms and for oxygens O_5 and O_9 are, however, considerably larger than the sum of the errors of the parameters, particularly for the y-coordinates and it is believed that these changes are significant with respect to the spontaneous polarization. The interpretation of these differences will be considered fully in a later section.

B. Room Temperature Structure

The total structure of colemanite as determined by the neutron diffraction study is illustrated in projection on the (001) and (010) planes in Figures 12 and 13, respectively. The basic framework agrees in every detail with that deduced from the x-ray work. Interatomic distances and inter-bond angles have been calculated for the boron - oxygen - calcium framework and appear in Table V. The distances between the calcium atom and oxygens, O_9 and O_2 each appear slightly longer than for the x-ray work. The differences

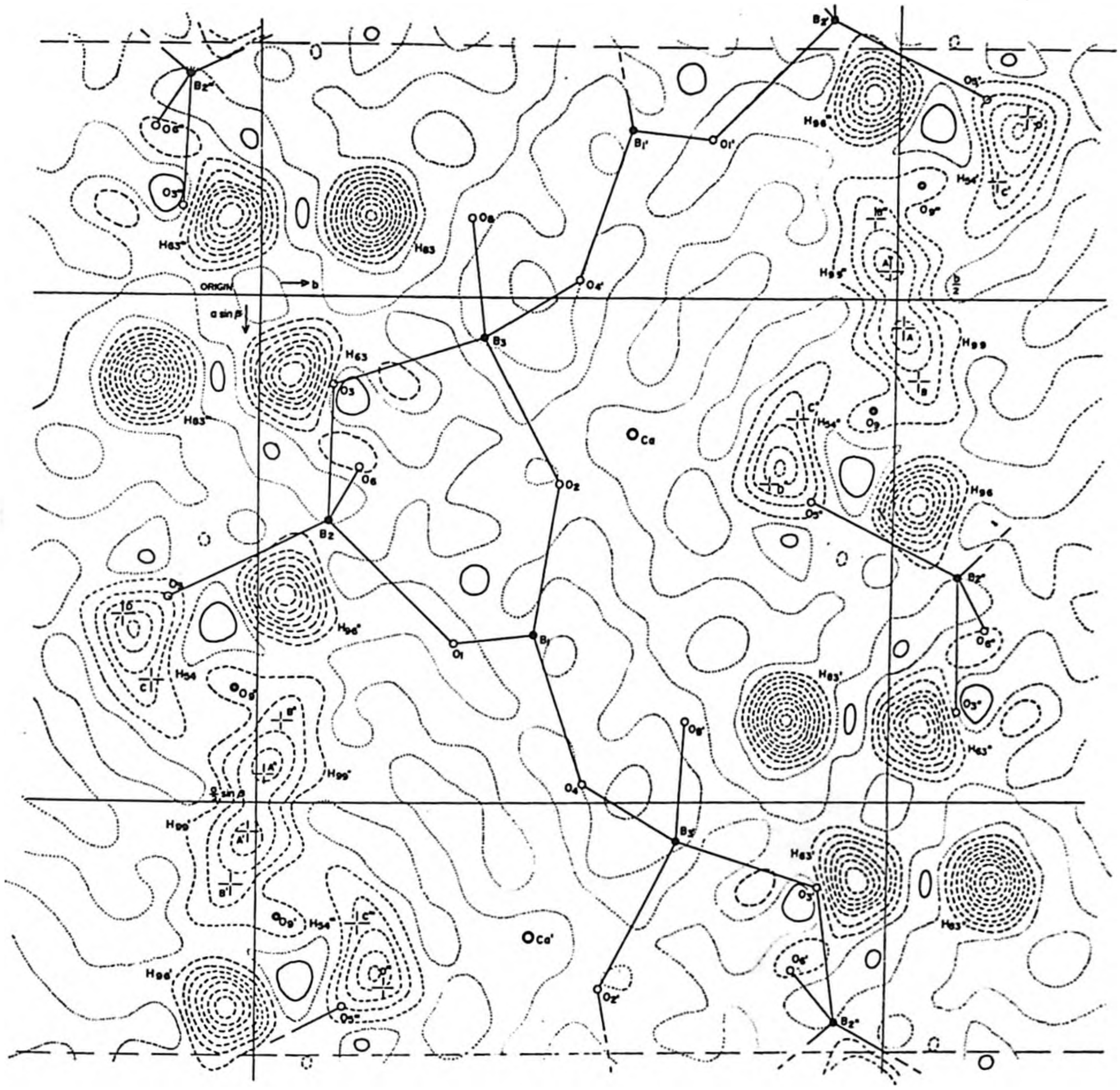

Figure 8. Fourier difference synthesis of the room temperature data showing only the hydrogen scattering projected on the (001) plane. Origin shown refers to space group $P2_1/a$.

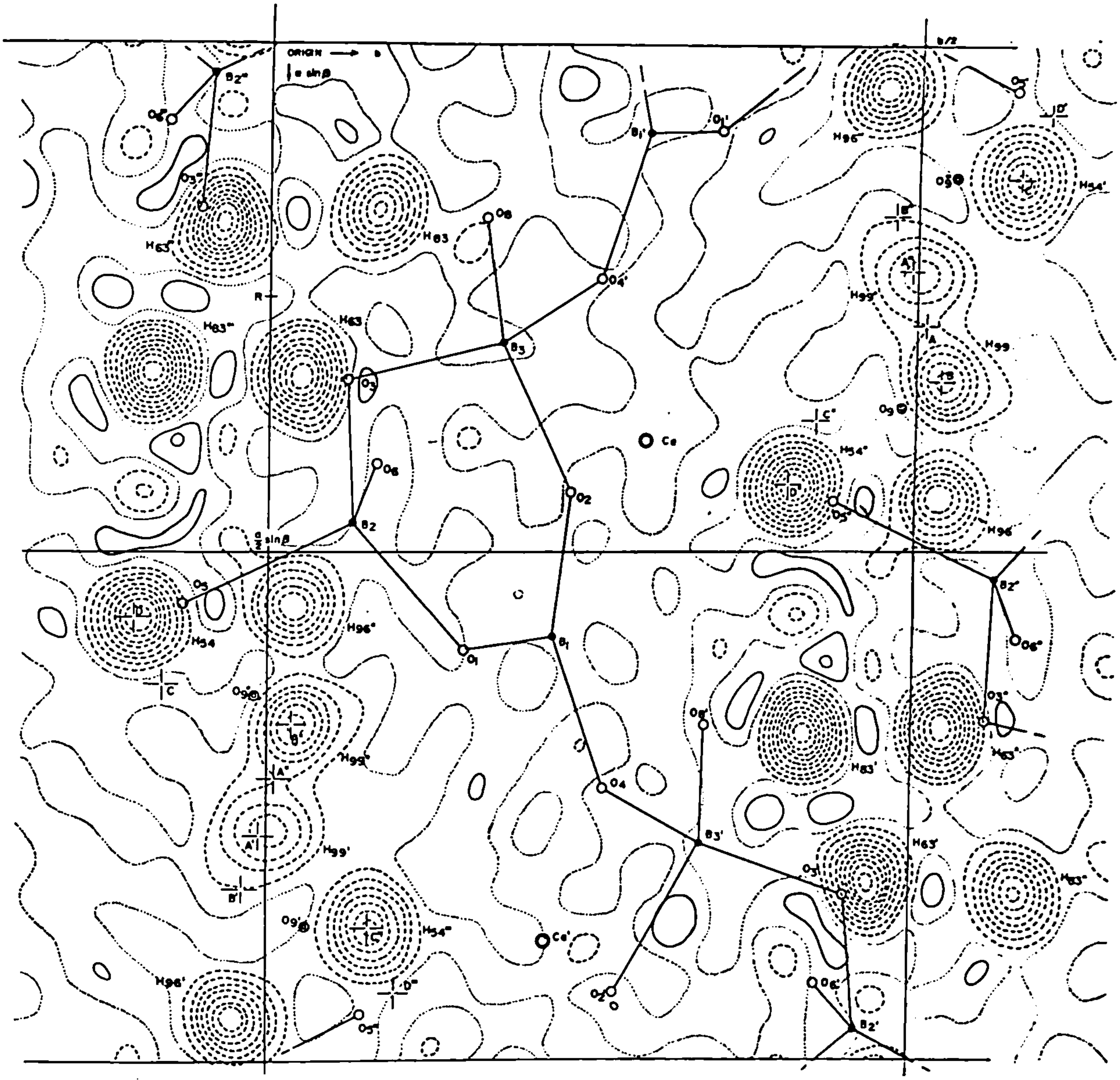

Figure 9. Fourier difference synthesis of the low temperature data showing only the hydrogen scattering projected on the (001) plane. Origin shown refers to space group $P2_1$; the room temperature origin is at the point "R". Points A, B, etc. are the respective room temperature positions of H_{99} and H_{54}.

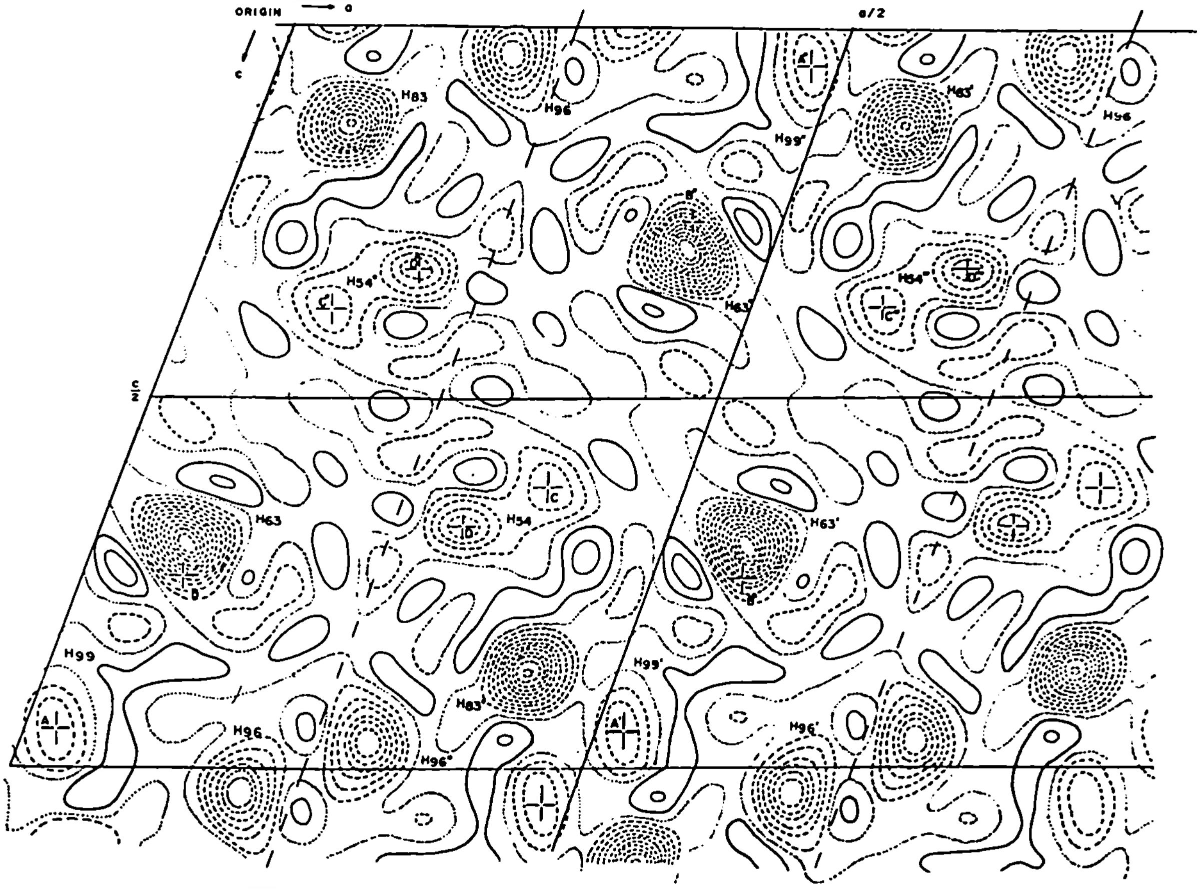

Figure 10. Fourier difference synthesis of the room temperature data showing only the hydrogen scattering projected on the (010) plane. Note that H_{99}-B and H_{63} are overlapped in this projection.

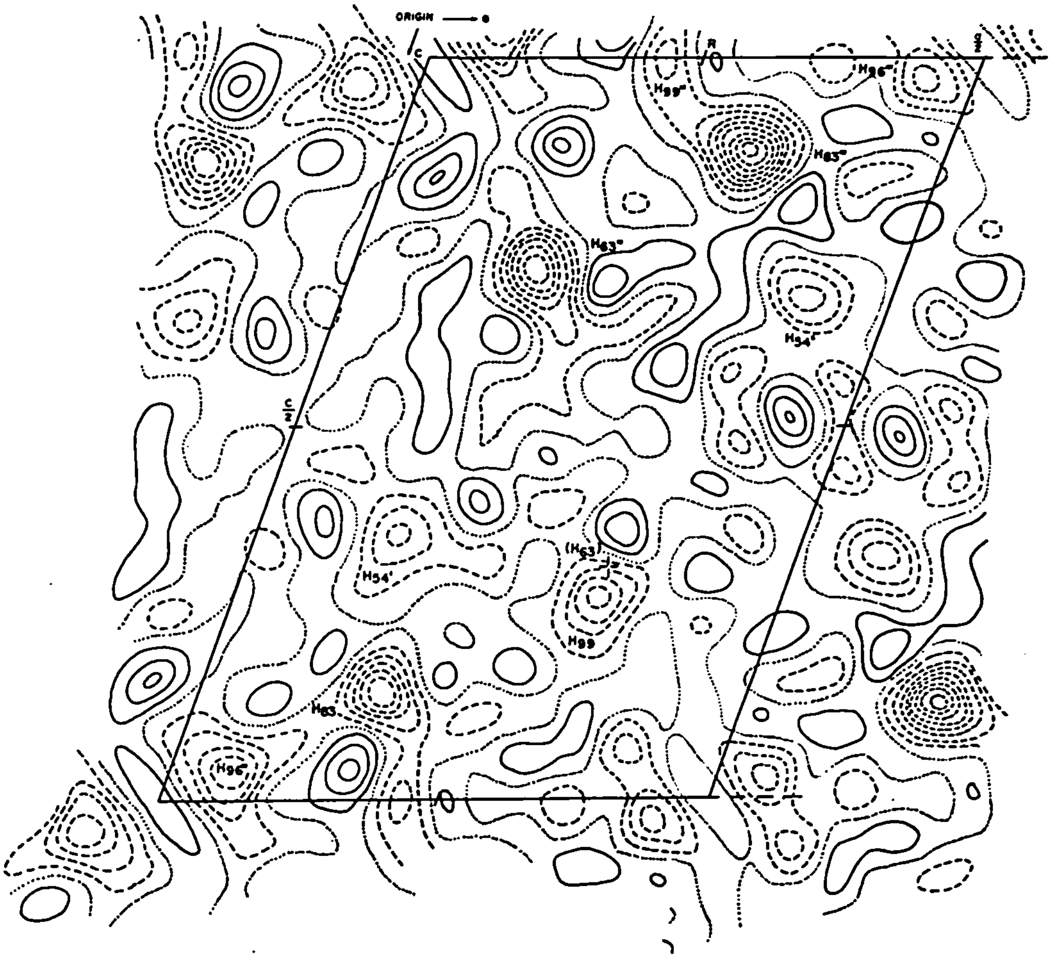

Figure 11. Fourier difference synthesis of the low temperature data showing only the hydrogen scattering projected on the (010) plane. The scattering of H_{63} has not been included so that H_{99} appears without overlap. The point "R" marks the origin of the room temperature plane group.

Figure 12. A projection on the (001) plane of the structure of colemanite above the ferroelectric transition temperature, showing the hydrogen positions as determined by the neutron diffraction study.

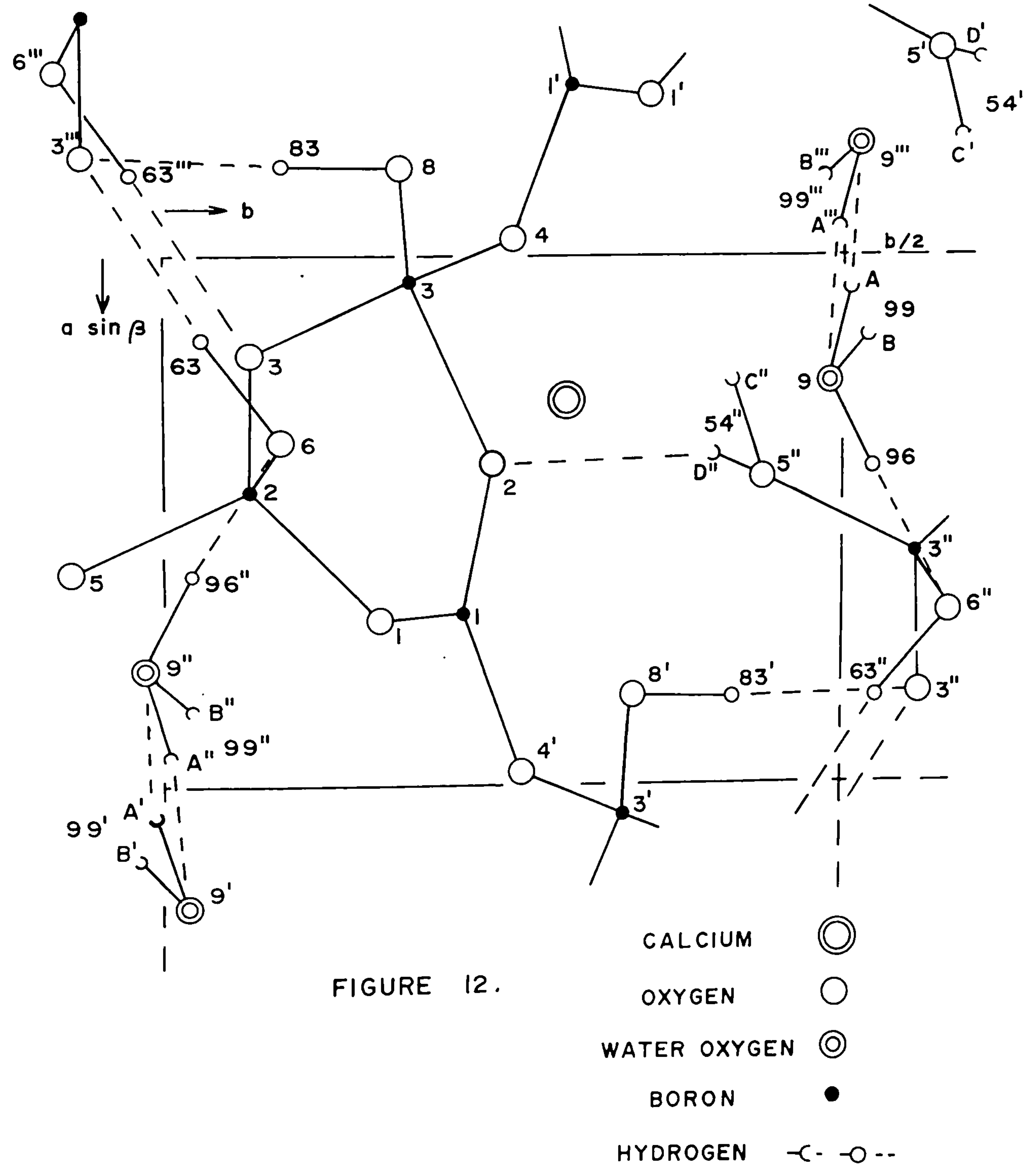
6'''
3'''
63'''
83
8
b
a sin β
63
3
6
2
5
96"
9"
B"
A"
99"
A'
99'
B'
9'
1
1'
1'
4
3
2
1
4'
8'
83'
3'
5'
D'
54'
C'
B'''
9'''
99'''
A'''
b/2
A
99
B
9
C"
54"
D"
5"
96
3"
6"
63"
3"
CALCIUM
OXYGEN
WATER OXYGEN
BORON
HYDROGEN

FIGURE 12.

Figure 13. A projection on the (010) plane of the structure of colemanite above the ferroelectric transition temperature, showing the hydrogen positions as determined by the neutron diffraction study. The large separation (1.58 Å) of the A and B positions of hydrogen H_{99} shows clearly in this projection.

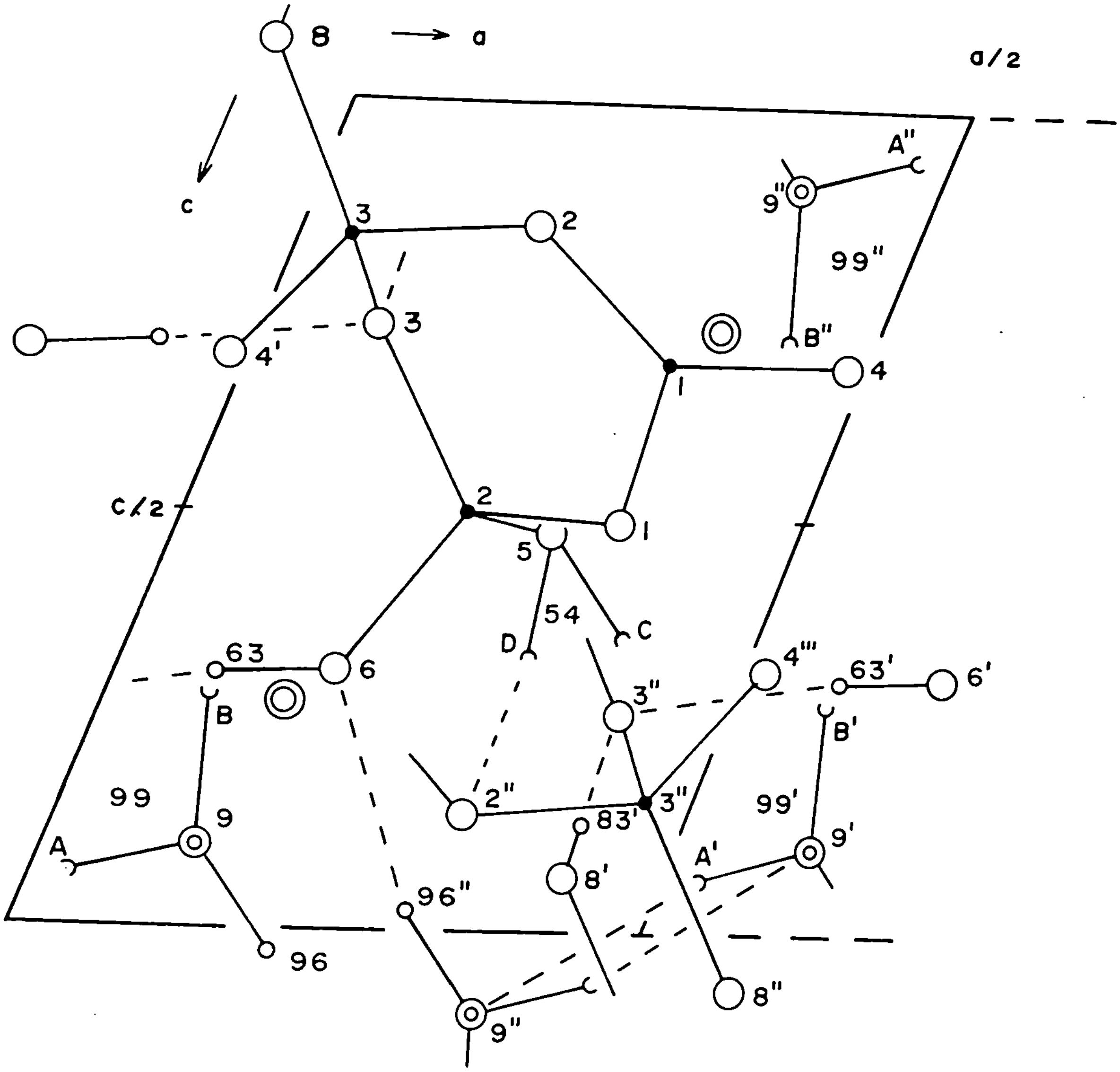

FIGURE 13.

CALCIUM ◎

OXYGEN ○

WATER OXYGEN ⊙

BORON ●

HYDROGEN —c - -
—o - -

TABLE V. INTERATOMIC DISTANCES AND INTERBOND ANGLES FOR THE ROOM TEMPERATURE STRUCTURE OF COLEMANITE. ERRORS QUOTED REFER TO THE LAST GIVEN FIGURE.

	NEUTRON DIFFRACTION THIS REFINEMENT		X-RAY DIFFRACTION CLARK ET AL. (1964).	
CALCIUM-OXYGEN DISTANCES (IN ANGSTROM UNITS)				
CA-O1'	2.548	± 10	2.556	± 6
CA-O2	2.452	9	2.420	5
CA-O4'	2.495	10	2.506	4
CA-O5''	2.441	14	2.449	6
CA-O6	2.419	10	2.426	5
CA-O8'	2.425	10	2.426	5
CA-O9	2.449	11	2.418	6
CA-O1'''	3.062 *	10	3.076 *	5
CA-O8	2.905 *	10	2.891 *	5
	-------		-------	
AVERAGE CA-O	2.467		2.457	
*THESE VALUES NOT INCLUDED IN AVERAGE				
BORON-OXYGEN DISTANCES WITHIN THE BORON GROUPS				
B1 (TRIANGLE)				
B1-O1	1.376	± 8	1.386	± 8
B1-O2	1.352	8	1.368	8
B1-O4	1.353	8	1.362	8
	-------		-------	
AVERAGE B1-O	1.360		1.372	
B2 (TETRAHEDRON)				
B2-O1	1.507	± 11	1.493	± 8
B2-O3	1.464	10	1.467	8
B2-O5	1.484	11	1.476	9
B2-O6	1.466	11	1.484	8
	-------		-------	
AVERAGE B2-O	1.480		1.480	
B3 (TETRAHEDRON)				
B3-O2	1.518	± 8	1.517	± 8
B3-O3	1.447	8	1.453	8
B3-O4'	1.466	8	1.478	8
B3-O8	1.473	8	1.454	8
	-------		-------	
AVERAGE B3-O	1.476		1.475	

TABLE V. (CONTINUED)

OXYGEN-BORON-OXYGEN ANGLES WITHIN THE BORON GROUPS

B1 (TRIANGLE) (ALL ANGLES + 0.8 DEGREES)

O1-B1-O2	120.1	120.8
O1-B1-O4	113.5	113.9
O2-B1-O4	126.4	125.3
	-------	-------
SUM	359.9	360.0

B2 (TETRAHEDRON)

O1-B2-O3	110.5	110.7
O1-B2-O5	111.8	111.0
O1-B2-O6	103.6	103.8
O3-B2-O5	106.8	106.7
O3-B2-O6	112.9	112.9
O5-B2-O6	111.4	111.7
	-------	-------
AVERAGE O-B2-O	109.5	109.5

B3 (TETRAHEDRON)

O2-B3-O3	108.5	109.0
O2-B3-O4'	107.3	107.2
O2-B3-O8	106.0	106.2
O3-B3-O4'	111.3	109.8
O3-B3-O8	112.4	113.2
O4'-B3-O8	111.1	111.4
	-------	-------
AVERAGE O-B3-O	109.4	109.4

BORON-OXYGEN-BORON ANGLES

WITHIN RING

B1-O1-B2	120.1	120.7
B1-O2-B3	117.9	117.0
B2-O3-B3	116.8	117.6

BETWEEN RINGS

B1-O4-B3'	136.4	136.7

are slight and may not be significant but it is noted that the neutron diffraction values are closer to the overall average. There are no significant differences observed for the B-O distances or for either the B-O-B or O-B-O angles.

The interatomic distances and inter-bond angles associated with the hydrogen atoms are shown in Table VI. These fall into two distinct groups; those associated with the "normal" hydrogen atoms H_{63}, H_{83} and H_{96}, and those associated with the "part-time" hydrogens H_{54} and H_{99}. For the former group we note that the O-H..O angles fall well within the range $167^\circ \pm 9^\circ$, cited as the average for 15 or more compounds examined by neutron diffraction techniques (Hamilton 1962, 1962A). For this group also, the B-O..O or O-O..O angles are between 87 and 117° so that strong bonds may be expected.

There are several factors which prevent hydrogen atoms H_{99} and H_{54} from entering into normal hydrogen bonds. The inversion centre between O_9 and O_9''' prevents H_{99A} from occupying a position in this bond permanently for reasons given earlier. Possible alternative acceptor atoms for the O_9-H_{99B} bond include the following: O_5', O_1', O_1'', O_4'' and O_5''. The O_9..O distances and O_6-O_9..O angles for these are listed in Table VI. We can see that for the first two the angles are not suitable and the distances are rather long for the next two. A linear bond with the last alternative would place the hydrogen atom closer than 2.4 Å from the calcium ion. Thus even an approximately linear bond is most unlikely and, from the actual position of this hydrogen atom, it would appear that it is not making a distinct bond with any of these atoms. It is directed toward a general region of negative charge but is probably most

TABLE VI. INTERATOMIC DISTANCES AND ANGLES PERTINENT TO THE HYDROGEN BONDS OF COLEMANITE AT ROOM TEMPERATURE. VALUES SHOWN IN PARENTHESES HAVE BEEN CORRECTED FOR THERMAL MOTION ACCORDING TO THE SCHEME OF BUSING AND LEVY (1964). ONLY CORRECTIONS GREATER THAN 0.01 A HAVE BEEN APPLIED. ERRORS QUOTED REFER TO THE LAST FIGURES GIVEN.

HYDROXYL O6-H63

DISTANCES (ALL LENGTHS IN ANGSTROM UNITS)

O6 - H63	0.992	± 20	(1.017 ± 31)
H63 - O3'''	1.773	15	(1.787 ± 19)
O6 - O3'''	2.759	11	
CA - H63	3.008	16	

ANGLES (ALL ANGLES ± 0.5 DEGREES)

B2-O6-O3'''	117.4
B2-O6-H63	112.8
O6-H63-O3'''	172.6
CA-H63-O6	45.5

HYDROXYL O8-H83

DISTANCES

O8-H83	0.962	± 18	(0.982 ± 23)
H83-O3'''	1.778	18	(1.789 ± 22)
O8-O3'''	2.734	8	
CA-H83'	2.756	20	

ANGLES

B3-O8-H83	108.1
B3-O8-O3'''	112.7
O8-H83-O3'''	171.7
CA-H83-O8	60.0

TABLE VI. (CONTINUED)

HYDROXYL O5-H54

DISTANCES (POSITION C)

O5-H54C	0.932	± 37	(0.980 ± 52)
H54C-O4'''	2.230	37	(2.250 ± 41)
O5-O4'''	2.807	13	
CA-H54C	2.728	36	(2.743 ± 43)
H54C-O9'	2.365	37	(2.383 ± 46)
O5-O9'	3.116	13	

ANGLES (ALL ANGLES ± 0.8 DEGREES)

B2-O5-O4'''	159.8
B2-O5-H54C	116.7
O5-H54C-O4'''	119.4
B2-O5-O9'	92.3
O5-H54C-O9'	137.4
CA-H54C''-O5''	62.4

DISTANCES (POSITION D)

O5-H54D	1.020	± 31	(1.036 ± 44)
H54D-O2''	2.211	29	
O5-O2''	3.064	12	
CA-H54D	2.992	30	

ANGLES

B2-O5-O2''	130.1
B2-O5-H54D	108.1
O5-H54D-O2''	140.1
CA-H54D''-O5''	48.6

TABLE VI. (CONTINUED)

WATER MOLECULE H96-O9-H99

DISTANCES

O9-H96	0.959	± 18	(1.003 ± 37)
O9-H99A	0.886	82	(0.97 ± 12)
O9-H99B	1.191	54	(1.236 ± 70)
H99A-O9'''	1.819	82	(1.860 ± 92)
H96-O6	1.833	18	(1.856 ± 30)
H99B-O5''	2.374	92	(2.397 ± 98)
O9-O6''	2.764	9	(2.771 ± 13)
O9-O9'''	2.662	10	(2.669 ± 14)
CA-H96	3.092	19	(3.106 ± 24)
CA-H99A	3.028	81	(3.053 ± 86)
CA-H99B	2.634	55	(2.651 ± 60)

ANGLES (ALL ANGLES ± 1)

O9'''-O9-O6''	86.8
O9'''-O9-H96	96.7
H99A-O9-O6''	94.3
H99A-O9-H96	102.8
H99B-O9-O6	129.2
H99B-O9-H96	119.7
O9-H96-O6''	162.9
O9-H99A-O9'''	158.1
O9-H99B-O5''	115.3
CA-H96-O9	40.9
CA-H99A-O9	42.5
CA-H99B-O9	67.9

POSSIBLE ALTERNATE ACCEPTORS FOR THE O9-H99B BOND

ANGLE		DISTANCE	
O6''-O9-O5''	122.1	O9-O5''	2.977
O6''-O9-O5'	136.3	O9-O5'	3.115
O6''-O9-O1''	103.5	O9-O1''	3.268
O6''-O9-O1'	169.9	O9-O1'	3.119
O6''-O9-O4''	90.1	O9-O4''	3.315

strongly influenced by O_5''. Unfortunately, because of the low scattering power of the "half atoms" coupled with the near overlap of H_{99B} and H_{63} in the (010) projection, the position of H_{99B} in particular is not as well defined as would be desirable. Neither the O_9-H_{99B} distance (1.191 Å) nor the H_{96}-O_9-H_{99B} angle (119.7°) are within the range of values* normally found for hydrogen bonds, and it is possible that this value is somewhat in error. A more complete discussion of the water molecules is given in the next section.

Turning to the O_5-H_{54} hydroxyl group we note some similarities with the former case. The possible acceptors for a hydrogen bond with O_5 are: O_4''', O_2'' and O_9'. The B_2-O_5-O angles shown in the Table indicate that O_2'' is the most likely acceptor although the O_5-O_4''' distance is smaller. The O_5-O_9' distance is too long to consider a bond as existing between these two atoms. Again, the presence of the calcium cation (Ca'' in this case) prevents a linear bond with O_2''. Thus, this hydrogen atom alternates between a weak bond with O_2'' (position 54D) and a position where it is influenced jointly by O_4''' and O_9' (position 54C). For both of these alternatives the B_2-O_5-H_{54} angle is about 112°.

C. The Polar Phase

The interatomic distances and interbond angles for the framework polyanions and the calcium coordination polyhedra obtained from

---

* In a recent summary of a number of neutron diffraction studies, Hamilton (1962A) has quoted O-H distances of up to 1.085 Å, although most of the values greater than 1.03 Å are associated with very short O..O distances.

the low temperature parameters are given in Table VII. Although the averages of the Ca-O and B-O distances have not changed, the individual deviations from these averages have increased somewhat. Some of these changes are definitely significant but, in general, the shifts are too small relative to the errors to discuss each change individually.

As expected, the hydrogen bond network does undergo significant changes which will be considered in detail. A complete list of the interatomic distances and angles involved in this network is given in Table VIII. The changes associated with the hydroxyl groups (except for O_5H_{54} and $O_5'H_{54}'$)are all rather small. We note that the linearity of the O_8'-H_{83}'..O_3'' bond has been reduced somewhat by the closer approach of the calcium cation to H_{83}'. The B_2'-O_8'-H_{83}' angle has also decreased from 108° at room temperature to 100° but there is a negligibly small increase in the O_8'..O_3'' distance.

The configuration of the two water molecules is illustrated in Figure 14 which is a projection of the atoms near a point of pseudo-symmetry on the (010) plane. It is clear from this diagram that the main result of the transition is a change in the state of the hydrogen atoms from dynamic symmetric disorder to reversible acentric order. Specifically, it may be noted that, relative to the room temperature values, both of the O_9'-H distances have increased and to some extent both O_9-H distances are shorter, although the O_9-H_{99} separation is still rather large. Neither of the H-O-H angles are appreciably different.

In general, when a water molecule in a solid is hydrogen bonded to other oxygen atoms, there is an inverse correlation

TABLE VII. INTERATOMIC DISTANCES AND INTERBOND ANGLES IN THE FRAMEWORK OF THE POLAR PHASE OF COLEMANITE. ERRORS QUOTED REFER TO THE LAST FIGURE GIVEN.

	UNPRIMED UNIT		PRIMED UNIT	
CALCIUM-OXYGEN DISTANCES (ALL CA-O DISTANCES ± 35)				
CA-O1'	2.632		2.501	
CA-O2	2.459		2.414	
CA-O4'	2.471		2.547	
CA-O5''	2.459		2.438	
CA-O6	2.395		2.465	
CA-O8'	2.370		2.478	
CA-O9	2.535		2.322	
CA-O8	2.985 *		2.798 *	
CA-O1	3.025 *		3.117 *	
AVERAGES	2.474		2.452	
* NOT INCLUDED IN AVERAGES				
BORON GROUPS				
B1 (TRIANGLES)				
B1-O1	1.439	± 40	1.383	± 35
B1-O2	1.298	40	1.384	35
B1-O4	1.347	40	1.314	35
AVERAGES	1.361		1.360	
B2 (TETRAHEDRA)				
B2-O1	1.439	± 38	1.592	± 40
B2-O3	1.483	39	1.443	40
B2-O5	1.516	47	1.412	45
B2-O6	1.396	39	1.526	43
AVERAGES	1.459		1.493	
B3 (TETRAHEDRA)				
B3-O2	1.483	± 36	1.532	± 36
B3-O3	1.476	36	1.443	36
B3-O4'	1.468	36	1.497	36
B3-O8	1.481	38	1.465	38
AVERAGES	1.477		1.482	

TABLE VII. (CONTINUED)

	UNPRIMED UNIT	PRIMED UNIT
OXYGEN-BORON-OXYGEN ANGLES (ALL ANGLES ± 1°)		
TRIANGLES B1,B1'		
B1-O1-B2	121.0	114.2
B1-O1-B4	109.6	114.5
B2-O1-B4	129.4	130.5
	-------	-------
SUMS	360.0	359.2
TETRAHEDRA		
O1-B2-O3	116.7	106.3
O1-B2-O	108.6	115.7
O1-B2-O6	109.4	95.5
O3-B2-O5	105.3	110.1
O3-B2-O6	108.5	114.0
O5-B2-O6	108.0	114.5
O2-B3-O3	109.8	108.3
O2-B3-O4'	112.2	102.4
O2-B3-O8	107.8	104.4
O3-B3-O4'	109.2	112.0
O3-B3-O8	106.0	117.2
O8-B3-O4'	111.7	111.1
	-------	-------
AVERAGES	109.4	109.3
OXYGEN-BORON-OXYGEN ANGLES		
WITHIN RING		
B1-O1-B2	117.7	120.9
B1-O2-B3	119.1	120.2
B2-O3-B3	110.8	121.5
BETWEEN RINGS		
B1-O4-B3'	133.0	
B1'-O4'-B3	136.0	

TABLE VIII. INTERATOMIC DISTANCES AND ANGLES PERTINENT TO THE HYDROGEN BONDS OF COLEMANITE IN THE POLAR PHASE. VALUES SHOWN IN PARENTHESES HAVE BEEN CORRECTED FOR THERMAL MOTION. ERRORS QUOTED REFER TO THE LAST FIGURES GIVEN.

	UNPRIMED UNIT			PRIMED UNIT		
HYDROXYL O6-H63						
O6-H63	0.987	± 48	(1.007)	1.029	± 46	(1.044)
O6-O3'''	2.763	38		2.756	37	
O3'''-H63	1.800	48		1.733	45	
CA-H63	3.055	46		2.948	45	
ANGLES (ALL ANGLES ± 1.5 DEGREES)						
B2-O6-O3'''	124.2			112.0		
B2-O6-H63	116.2			111.3		
O6-H63-O3'''	164.2			172.6		
HYDROXYL O8-H83						
O8-H83	0.927	± 47	(0.945)	0.959	± 44	(.973)
O8-O3'''	2.653	41		2.764	34	
H83-O3'''	1.730	47		1.826	44	
CA-H83	2.718	45		2.783	43	
ANGLES						
B3-O8-O3'''	117.4			108.3		
B3-O8-H83	118.0			99.9		
O8-H83-O3'''	174.4			165.3		

TABLE VIII. (CONTINUED)

HYDROXYL O5-H54

O5-H54	1.028	± 48	(1.047)
O5-O2''	3.142	44	
H54-O2''	2.277	39	
CA''-H54	2.978	38	
O5-O4'''	2.807	46	
H54-O4'''	2.479	40	

O5'-H54'	0.957	48	(0.990)
O5'-O4''	2.805	46	
O5'-O9	3.113	45	
O5'-O2'''	3.020	42	
H54'-O9	2.283	47	
H54'-4''	2.311	44	
H54'-2''	2.627	44	
CA'''-H54'	2.827	41	

ANGLES (ALL ANGLES ± 1.5 DEGREES)

B2-O5-H54	110.6
B2-O5-O2''	131.9
O5-H54-O2''	140.8
B2-O5-O4'''	161.1
O5-H54-O4'	97.6
B2-O5-O9'	92.2
O5-H54-O9'	95.2

B2'-O5'-H54	109.6
B2'-O5'-O4''	159.6
B2'-O5'-O9	92.2
O5'-H54'-O2'''	105.0
O5'-H54'-O9	144.7
O5'-H54'-O4''	111.4
B2'-O5'-O2'''	133.8

TABLE VIII. (CONTINUED)

WATER MOLECULES

O9-H96	0.929	± 74	(0.983)
O9-H99	1.070	52	(1.100)
O9-O6''	2.862	39	
O9-O9'''	2.674	41	
O6''-H96	1.982	72	
O9-O5''	2.978	46	
O9-O1''	3.200	39	

O9'-H96'	1.037	54	(1.062)
O9'-H99'	1.003	73	(1.053)
O9'-O6'''	2.716	42	
O6'''-H96'	1.702	52	(1.717)
O9''-H99'	1.737	51	(1.751)

CA-H96	3.038	72
CA-H99	2.720	51
CA'-H96'	3.095	53
CA'-H99'	2.905	71
H99-O5''	2.333	57
H99-O5'	2.452	54
H99-O1''	2.253	50
H99-O1'	2.875	48
H99-O4''	2.655	51

ANGLES (ALL ANGLES ± 2 DEGREES)

O9''-O9'-O6'''	85.4
O6'''-O9-O5''	122.4
H99-O9-H96	118.9
O9-H96-O6''	157.4
O9-H99-O5''	117.2
O9-H99-O1''	146.5

O9'-H96'-O6'''	165.1
O9'-H99'-O9''	153.9
H99'-O9'-H96'	104.4

Figure 14. Configuration of the water molecules in the polar phase of colemanite. The two molecules shown are related by the centre of symmetry in the non-polar phase. Atoms whose designations differ by two primes are related by the screw axis in both phases. Note that the origin for the low temperature space group is on the 2_1 axis, whereas the origin for the high temperature space group is at $\bar{1}$, a difference of a/4.

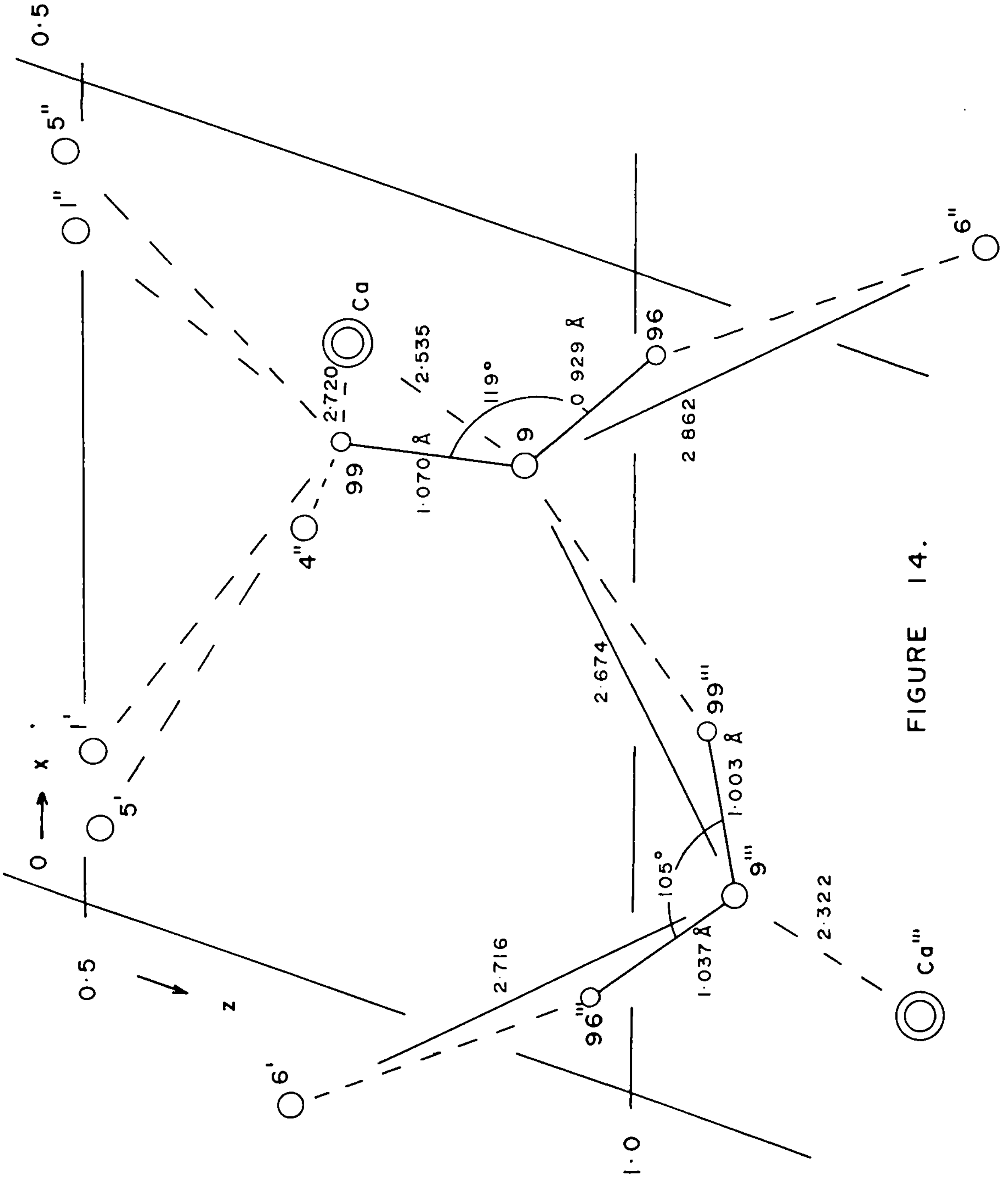
0·5
5''
1''
Ca
2·720
2·535
119°
0 929 Å
96
6''
9
99
1·070 Å
2 862
4''
2·674
99'''
1·003 Å
9'''
1'
5'
0 → x
0·5
z
105°
2·716
1·037 Å
2·322
Ca'''
96''
6'
1·0

FIGURE 14.

observed between the O-H distance and the O..O separation. Thus the increased O_9'-H distances in the polar phase are compatible with the decrease in O_9'-O_6''' and O_9'-O_9'' separations observed for the primed water molecule. In the unprimed unit the decreased O_9-H_{96} distance follows from an increase in the O_9-O_6'' separation, but the lengthened O_9-H_{99} distance and larger H_{96}-O_9-H_{99} angle are not as easily understood.

The value observed for the H-O-H angle in a free water molecule is 104.5° but in a solid this angle is found to vary over a considerable range* depending on the nearest neighbours of the water molecule on the side remote from the hydrogen atoms. It is mainly the p-orbitals of the oxygen atom which are used to bond the hydrogen atoms but the admixture of some s-character opens the H-O-H angle from 90° (pure p-bonding) to its observed value. This exchange of p and s character between the bonding electrons and the lone pairs may be enhanced by the close approach of an electropositive atom to the region of the lone pair orbitals and in the extreme case may lead to full sp^2 hybridization (as for example the hydronium ion, OH_3^+, or in the tunellite polyion, see Figure 1).

For the O_9' water oxygen the only close cation is the calcium atom at a distance of 2.322 Å and the H-O-H angle is 105°. For O_9, on the other hand, H_{99}''' is only 1.737 Å distant and the calcium cation is at 2.535 Å separation. The close approaches of these

---

* The mean value of the H-O-H angle in solids is about 110° with a standard deviation of 4°. See, for example, Bacon and Curry, (1962) on $CuSO_4.5H_2O$.

cations probably account largely for the H-O-H angle of 119°.

Since H_{99} is apparently not involved in a unique bond, the expected O_9-H_{99} distance should be less than 1.0 Å and, to account for the larger value observed, we note that H_{99} is in a position where it is influenced by five oxygen atoms at distances of 2.25 to 2.88 Å. The presence of H_{99} has a negligible effect in reducing the distance of any of these oxygen atoms to O_9 but it is quite reasonable to postulate that there is a strong effect of these oxygens in determining the position of H_{99}.

The relationship of hydroxyl O_5H_{54} to the water molecule and the calcium cation is illustrated in Figure 15. The primed and unprimed water-hydroxyl networks are shown separately, projected on the (100) plane. The hydrogen atoms of these hydroxyl groups also have undergone an ordering process at the transition temperature. Hydrogen H_{54} is nearly in the position labelled D in the room temperature structure, in which it is making a very weak bond with oxygen O_2'', whereas H_{54}' is approximately in the C' position and the C and D' positions are unoccupied. Although, in the C' position, it cannot be considered to be bonding O_5'' to either O_9' or O_4''', the position of hydrogen H_{54} is strongly influenced by the presence of these two oxygen atoms. The quantities which are most important in determining the positions of these hydrogen atoms are the B_2-O_5-H angles and the Ca-H distances. The significance of the relative positions assumed by the hydrogen atoms in the polar phase will be considered in the next chapter.

Figure 15. (a) The unprimed water-hydroxyl network projected on the (100) plane. The separations of the calcium atom and the hydrogen atoms are indicated. The displacement of the calcium atom from its room temperature position is also shown.

(b) As above, for the primed network. Atoms whose designations differ by two primes are screw-axis related, hence doubly primed atoms are considered part of the unprimed system, and triply primed atoms part of the primed system.

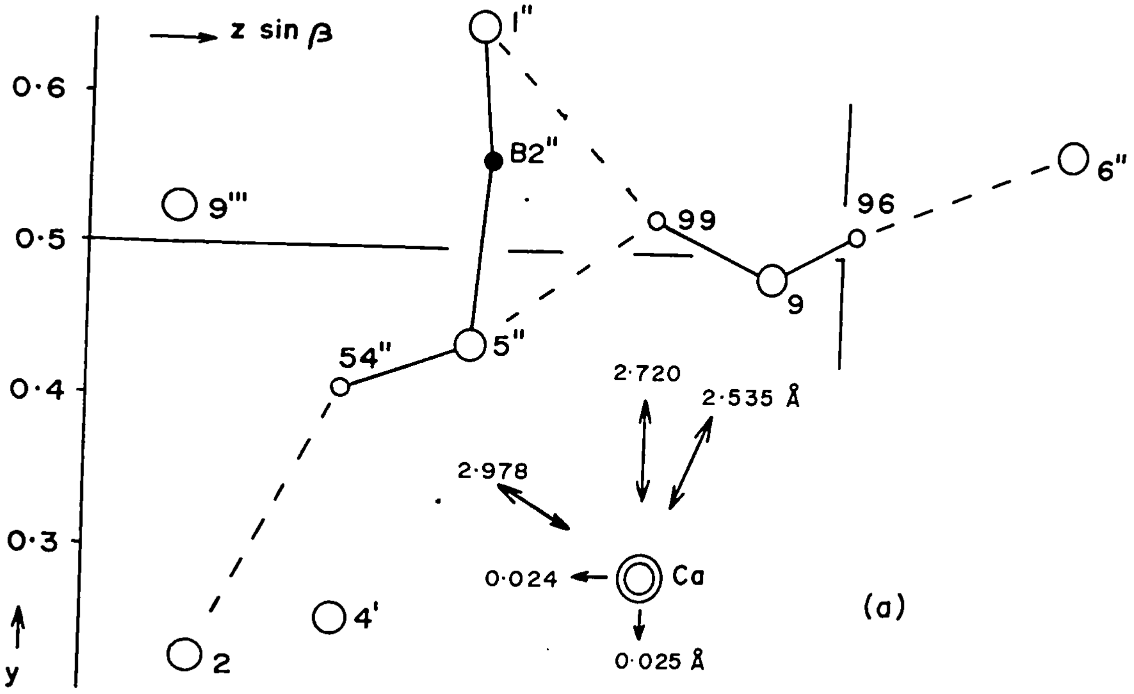

z sin β
0·6
0·5
0·4
0·3
y
1"
B2"
9'''
99
96
6"
9
5"
54"
2·720
2·535 Å
2·978
Ca
0·024
0·025 Å
(a)
2
4'

FIGURE 15.

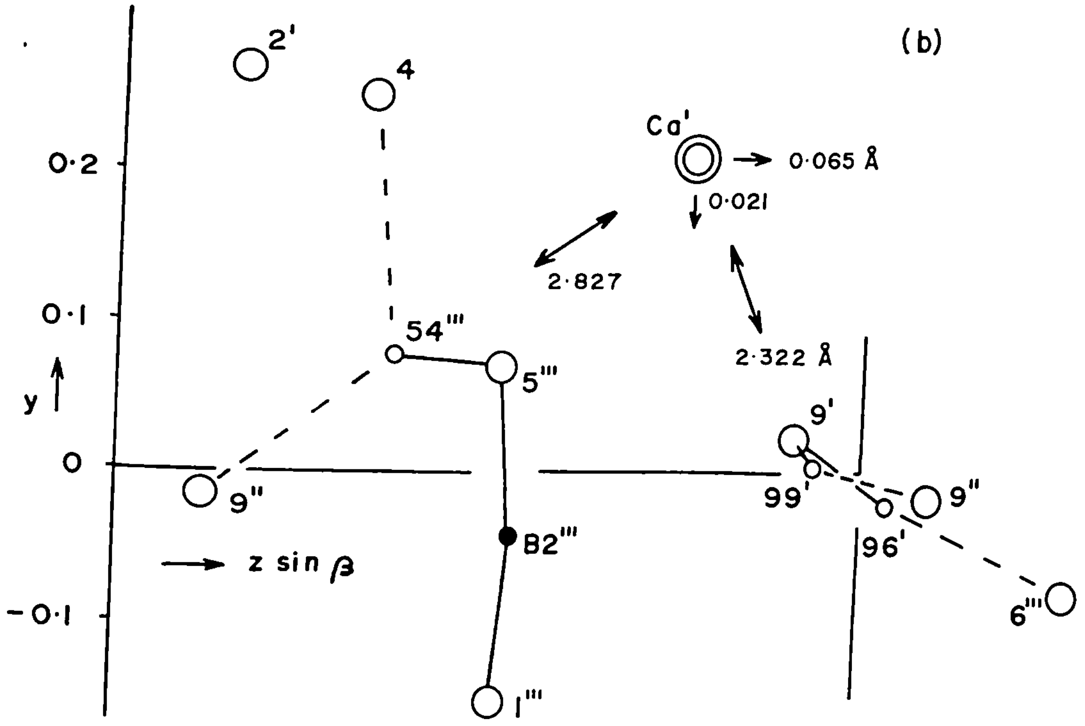

(b)
2'
4
Ca'
0·065 Å
0·021
0·2
2·827
0·1
54'''
5'''
2·322 Å
y
9'
0
99'
9"
9"
96'
B2'''
z sin β
-0·1
6'''
1'''

V. CONCLUSIONS

A. The Spontaneous Polarization

The net electric dipole moment which is characteristic of ferroelectric materials does not, in general, arise from the reorientation of distinguishable dipoles (as in the magnetic analog) but rather from a net separation of the centroids of the positive and negative charge.

In colemanite the net dipole moment appears to arise from slight displacements of all the atoms from strict glide-plane symmetry. Since the screw axis symmetry element is retained in the polar phase, the effect of all deviations from the room temperature positions cancel except those in the y-direction -- hence the polar axis. If reasonable assumptions can be made regarding the magnitudes and signs of the charges residing on each atom, the magnitude of the dipole moment can be calculated as; $P_s = N_c \sum_i q_i \delta y_i$, where N_c is the number of unit cells per unit volume, q_i is the effective charge on each ion and δy_i is the shift of the ion from its centrosymmetric position and the sum is over all atoms in the unit cell.

The charge distribution for the polyanion was considered in a previous section and for the hydrogen bonds, we have assumed 40% ionic character placing -0.34e on the donor oxygen and -0.06e on the acceptor(s). The following total charge assignments were made: Ca, +2.00e; B_1, +0.72e; B_2,B_3,+1.32e; O_1, -0.83e; O_2O_4, -0.85e;

O_3, -1.27e; O_5, -0.93e; O_6, -0.97e; O_8, -0.91e; O_9, -0.75e; all hydrogen, +0.40e. With $N_c = 1.77 \times 10^{21}$ unit cells/cm^3 and using the displacements as given in Table IV, the value for $P_s = 0.501\ 10^{-6}$ Coul/cm^2 was obtained. The close agreement with the measured value of 0.45×10^{-6} Coul/cm^2 at -20°C is probably fortuitous, but the fact that the observed displacements give the correct order of magnitude is quite significant.

The direction of this polarization with respect to the external electric field cannot be obtained from the usual diffraction data since only intensities are measured. However, when a crystal contains one or more atoms which are strong absorbers of the incident radiation, the scattering for those atoms is not exactly in phase or exactly 180° out of phase with the incident beam and the relationship $F_{hk\ell} = F_{\bar{h}\bar{k}\bar{\ell}}$, known as Friedel's Law, does not hold for non-centrosymmetric distributions of the absorbing atoms. This result may be seen from the expression for the structure factor:

$$F_{hk\ell} = \sum_j b_j\ e^{2\pi i(hx_j+ky_j+\ell z_j)} \equiv \sum_j b_j\ e^{i\alpha_j}$$

But if $b_j = b_j' + ib_j'' \equiv b_j e^{i\delta}$ as it is for an absorbing nuclide

then; $F_{hk\ell} = \sum_j b_j\ e^{i(\alpha_j+\delta)}$ and $F_{\bar{h}\bar{k}\bar{\ell}} = \sum_j b_j\ e^{i(-\alpha_j+\delta)}$.

In this case $F_{hk\ell} \cdot F_{hk\ell}^* \neq F_{\bar{h}\bar{k}\bar{\ell}} \cdot F_{\bar{h}\bar{k}\bar{\ell}}^*$ which result is sometimes known as a Bijvoet inequality.

The imaginary component of the boron scattering length has recently been measured to be 0.021×10^{-12} cm by Peterson and Smith, (1962) and the real part is known from this study to be 0.51×10^{-12} cm.

This complex scattering length may be used to relate the direction of the boron displacements with the crystallographic axes of the sample crystal and hence with the direction of the external electric field. To do this, the intensity of a particular reflection ($I_{hk\ell}$, say) and its negative, $I_{\bar{h}\bar{k}\bar{\ell}}$ are measured with the direction of the electric field (+) along the polar axis of the sample crystal chosen to be the positive direction. These measurements are repeated with the field reversed (-) and the sign of the difference $(I_{hk\ell}^{+} + I_{\bar{h}\bar{k}\bar{\ell}}^{-}) - (I_{hk\ell}^{-} + I_{\bar{h}\bar{k}\bar{\ell}}^{+})$ may be compared with the calculated differences in $F_{hk\ell}$ and $F_{\bar{h}\bar{k}\bar{\ell}}$. Any differences between $I_{hk\ell}$ and $I_{\bar{h}\bar{k}\bar{\ell}}$ due to the geometry of the crystal or other effects will cancel.

For the (0, 10, 0) reflection in colemanite the calculated value for the above difference was 1.5% of the integrated intensity. However, after several remeasurements of the four peaks, the accumulated difference was only 0.33 ± 0.39%. Since the value obtained was smaller than the error involved, the sign of the difference cannot be considered significant. If it were to be considered significant the field of the calculated dipole moment would be the same as the external field. This would place the assignment of the charges in considerable doubt.

A more likely reason for this low result is that the polarity of the sample was not reversed by the external field. It was noted earlier that many samples of colemanite had very biased hysteresis loops indicating some degree of polarity clamping from impurity space charges. The fields due to these internal charges may, in some cases, be as high as 50 kv/cm (Wieder, 1959). The maximum field which could be applied to the colemanite sample without damaging the crystal support gave a field of only 10 kV/cm. It is therefore quite possible that the polarity of the dipole moment was determined only by the internal fields. It is hoped that an opportunity to continue the search for these inequalities will exist in the near future.

B. Transition Mechanism

On the basis of the observed differences between the polar and non-polar structures, a model for the mechanism of the transition may be proposed. Figure 15 shows that there is a strong interdependence between the stabilities of the positions of the calcium cation and the water hydrogen H_{99}. Above the transition temperature these hydrogen atoms have sufficient energy to jump the barrier between the A and B positions resulting in a dynamically disordered state. As the temperature is lowered, one of these hydrogen atoms may settle into one or the other of the two alternative positions. The relative stability of the two states for the inversion-related atom will then be changed such that it settles in the non-equivalent alternative position. The effect of this ordering on the calcium neighbours of each of these hydrogen atoms is such that they move toward or away from the water oxygens, in a sense, "following" the hydrogen atoms. The influence of this relaxation is spread to the nearby polyanion chains through the hydroxyl, O_5H_{54}. The strength of the interactions throughout the water-calcium-hydroxyl-polyanion network is sufficient to ensure that the ordering of one cell exerts a strong influence on the neighbouring cells to become ordered with the same relative configuration.

Conversely, as the temperature of a crystal in the polar phase is raised, the thermal energy of the hydrogen atoms becomes sufficient to make the B position of H_{99} unstable. Once one hydrogen jumps the barrier to the A position, the water hydrogen nearest to it (pseudo-inversion related) is forced into its B position and this disordering influence spreads in a like manner. In this case, however, neither position is stable and the exchange of positions is rapidly repeated.

We have seen that colemanite, in its polar phase, is non-centrosymmetric and that the magnitude of the displacements from centrosymmetry lead to a non-zero value of the dipole moment. This implies that the crystal is pyroelectric, but the criterion for ferroelectricity is that this dipole moment must be reversible. To accomplish this reversal, the bistable hydrogen atoms must be moved from the A and C positions to the B and D positions (or vice versa) and the other atoms must undergo certain displacements, which, as Table IV has shown, are relatively small. The switching of the hydrogen atoms does not require the breaking of any strong bonds but only the rearranging of rather weak hydrogen bonds. Consequently, the energy required to switch the structure from one state to the other is quite small and the reversal may be accomplished with the application of an electric field considerably weaker than that which will cause dielectric breakdown.

In this model, a possible reason for the effect of the size of the cation on the temperature at which the disordering begins may be suggested. The strontium ion is larger than the calcium ion and will prefer to be coordinated by eight or nine oxygen atoms. The two neighbours of calcium at 2.9 and 3.1 Å will likely move in slightly, as the others move out to make a larger cation polyhedron. This would decrease the electrostatic pressure on the hydrogen positions through a screening effect, allowing the polar phase to exist to a somewhat higher temperature. Unfortunately, no crystallographic data is available for the strontium isomorph of colemanite so that it is not known to what extent the volume of the unit cell is increased. It is likely to increase somewhat since the atoms in colemanite are very closely packed. In a reverse manner, the substitution of the smaller magnesium ion would leave the hydrogen atom more exposed to the cation polyhedron and thus increase the pressure on the water hydrogen (assuming a proportionate decrease in the cell volume). On the other hand, without a change in cell volume, a smaller ion would be able to shift further away from the water molecule, in which case the magnitude of the spontaneous polarization would be smaller.

REFERENCES

Bacon, G. E. (1962). Neutron Diffraction, 2nd ed. Oxford, Clarendon Press.

Bacon, G. E. (1962). J. Phys. Soc. Japan, 17, Suppl. B-11, 324.

Bacon, G. E. and Curry, N. A. (1962). Proc. Roy. Soc. (London) A, 266, 95.

Blinc, R., Maricic, S. and Pintar, M. (1960). Croatica Chem. Acta 32, 67.

Busing, W. R., Martin, K. O. and Levy, H. A. (1962). Oak Ridge National Laboratory, Technical Manual, TM-305.

Busing, W. R. and Levy, H. A. (1964). Acta Cryst. 17, 142.

Christ, C. L. (1953). Amer. Min. 38, 411.

Christ, C. L., Clark, J. R. and Evans, H. T. (1954). Acta Cryst. 7,453.

Christ, C. L., Clark, J. R. and Evans, H. T. (1958). Acta Cryst. 11,761.

Christ, C. L. (1960). Amer. Min. 45, 334.

Chynoweth, A. G. (1957). Acta Cryst. 10, 511.

Clark, J. R. (1964). Amer. Min. 49, 1549.

Clark, J. R. Appleman, D. E. and Christ, C. L. (1964). J. Inorg. Nucl. Chem. 26, 73.

Davisson, J. W. (1956). Acta Cryst. 9, 9.

Edwards, J. O. and Ross, V. (1960). J. Inorg. Nucl. Chem. 15, 329.

Goldsmith, G. J. (1956). Bull. Am. Phys. Soc. Ser. II. 1, 322.

Hamilton, W. C. (1962). J. Phys. Soc. Japan 17, Suppl. B-11, 374.

Hamilton, W. C. (1962A). Ann. Rev. Phys. Chem. 13, 19.

Hamilton, W. C. (1963). Acta Cryst. 16, 609.

Hauptman, H. and Karle, J. (1953). Solution of the Phase Problem. I. A C A Monograph No. 3. Wilmington: The Letter Shop.

Holuj, F. and Petch, H. E. (1958). Can. J. Phys. **36**, 145.

Holuj, F. and Petch, H. E. (1960). Can. J. Phys. **38**, 515.

International Tables of X-ray Crystallography (1962). Vol. II.

Pauling, L. (1960). The Nature of the Chemical Bond. (Cornell Univ. Press).

Perloff, A. and Block, S. (1960). Amer. Min. **45**, 229.

Petch, H. E., Brouwer, W., Torrie, B. H. and Brown, I. D. (1960). Res. Reactor J. **1**, 8.

Peterson, S. W. and Smith, H. G. (1962). J. Phys. Soc. Japan **17**, Suppl. B-11, 335.

Torrie, B. H. (1963). Doctoral Thesis, McMaster Univ.

Torrie, B. H., Brown, I. D. and Petch, H. E. (1964). Can. J. Phys. **42**, 229.

Wieder, H. H. (1959). J. Appl. Phys. **30**, 1010.

Wieder, H. H., Clawson, A. R. and Parkerson, C. R. (1962). J. Appl. Phys. **33**, 1720.

Wieder, H. H., Clawson, A. R. and Parkerson, C. R. (1963). Bull. Am. Phys. Soc. Ser. II, **8**, 269.

APPENDIX 1

The basic problem of crystal structure refinement by the least squares criterion may be stated in the following way: Given a set of observations ($|F_j^o|$)with relative weights w_j, find a set of positional and thermal parameters (P_i) for which the quantity,

$$R(P_i) = \sum_j w_j \left(\left|F_j^o\right| - \left|F_j^c(P_i)\right| \right)^2 \text{ is a minimum.}$$

The quantities F_j^c are well known functions of the (P_i). The quantities to be determined are the set (δP_i) such that the set $(P_i^o + \delta P_i) = (\hat{P}_i)$ where (P_i^o) is the set of trial parameters and the set ($\hat{P}_i$) minimizes R. The (δP_i) are introduced in the expression for R by the Taylor expansion of the F_j^c;

$$F_j^c\,(\hat{P}_i) = F_j^c\,(P_i^o) + \sum_i \frac{\partial F_j^c}{\partial P_i}\,\delta P_i + \ldots$$

where terms in δP of quadratic and higher order are neglected.

We define $D_j(P_i) = w_j \left\{ F_j^o \left[\dfrac{F_j^c(P_i)}{|F_j^c(P_i)|} \right] - F_j^c(P_i) \right\}$

The (δP_i) may be obtained from the simultaneous solution of the set of equations obtained by setting the variation of R with respect to the (δP_i) equal to zero:

$$\frac{\partial R}{\partial \delta P_k} = 2 \sum_j \left\{ D_j(P_i) - \sum_i w_j \frac{\partial F_j^c(P_i)}{\partial P_i}\,\delta P_i \right\} \frac{\partial F_j^c(P_i)}{\partial P_k} = 0$$

These "normal" equations may be written in matrix form: $A \cdot \overrightarrow{\delta P} = \vec{B}$ where the elements of the matrix A and the components of the vector $\vec{B}$ are respectively;

$$A_{ik} = \sum_j w_j \frac{\partial F_j^c(P_i)}{\partial P_i} \cdot \frac{\partial F_j^c(P_i)}{\partial P_k}$$

$$B_k = \sum_j D_j(P_i) \cdot \frac{\partial F_j^c(P_i)}{\partial P_k}$$

The solution of the matrix equation lies in finding the inverse matrix, A^{-1}, such that $A^{-1} A \overrightarrow{\delta P} = \overrightarrow{\delta P} = A^{-1}\vec{B}$. The set $(P_i + \delta P_i)$ is as close to the set $(\hat{P}_i)$ as the assumptions made in the Taylor expansion permit.

The computer program adapted from that of Busing, Martin and Levy (1962) by members of this crystallography group, especially J. S. Stephens, allows the simultaneous adjustment of up to 140 parameters using up to 1500 observations of F^o.

The estimated standard errors quoted for the corrected parameters are the quantities:

$$\sigma(\delta P_i) = \frac{\left(\sum_j w_j (F_j^o - F_j^c)^2\right)^{1/2}}{(NO - NV)} \cdot A^{-1}_{ii} \text{ where}$$

NO is the number of observations, NV is the number of parameters to be adjusted and the A^{-1}_{ii} are the diagonal elements of the inverse matrix A^{-1}.

APPENDIX 2

TABLE A-1. ROOM TEMPERATURE OBSERVED AND CALCULATED STRUCTURE FACTORS. DATA ARE LISTED IN ORDER OF INCREASING BRAGG ANGLE.

(HK0) DATA

H	K	L	OBS	CALC
1	1	0	17.10	17.88
0	2	0	91.52	-81.42
1	2	0	46.77	-46.11
2	0	0	32.34	-32.33
2	1	0	11.01	-12.49
1	3	0	18.76	-17.50
2	2	0	41.29	-40.35
0	4	0	23.84	24.57
2	3	0	43.77	-43.03
1	4	0	4.51	-5.57
3	1	0	8.02	7.48
3	2	0	8.04	-8.82
2	4	0	6.33	-5.75
3	3	0	51.05	-50.16
1	5	0	5.69	-8.14
4	0	0	31.48	-32.32
4	1	0	15.82	17.18
2	5	0	98.82	-98.91
3	4	0	34.30	-35.20
4	2	0	7.87	-6.51
0	6	0	27.41	-26.64
1	6	0	2.82	-2.54
4	3	0	2.88	-3.13
3	5	0	56.74	56.44
2	6	0	43.43	43.51
4	4	0	8.19	-2.75
5	1	0	29.82	27.15
1	7	0	4.87	-2.86
5	2	0	24.52	21.90
3	6	0	20.07	19.98
4	5	0	63.09	60.57
5	3	0	36.51	34.41
2	7	0	18.28	-13.06
5	4	0	9.02	-11.47
0	8	0	60.81	-60.60
1	8	0	42.64	41.73
3	7	0	27.14	27.39
4	6	0	47.18	-47.48
6	0	0	61.51	61.86
6	1	0	22.10	-20.20
2	8	0	31.79	31.43
6	2	0	53.49	-50.62
5	5	0	30.01	30.20
6	3	0	40.14	-39.83
4	7	0	7.85	-13.85
3	8	0	26.13	25.70
1	9	0	56.95	-58.18
5	6	0	19.53	-18.14
6	4	0	26.67	22.65
2	9	0	26.31	29.80
6	5	0	4.30	-3.16
7	1	0	30.42	-30.89
4	8	0	7.00	1.66
5	7	0	2.89	-1.33
7	2	0	44.84	-44.53
3	9	0	4.10	-5.61
0	10	0	93.68	-95.52
7	3	0	38.01	40.45
1	10	0	14.09	13.87
6	6	0	46.64	-49.38
2	10	0	8.78	-9.93
7	4	0	62.55	62.78
5	8	0	15.38	-9.94
4	9	0	20.60	19.12
6	7	0	25.22	-26.99
3	10	0	58.54	59.15
7	5	0	58.88	-58.62
8	0	0	15.66	-15.68
8	1	0	29.30	29.38
1	11	0	10.29	6.87
8	2	0	27.39	28.33
5	9	0	61.06	60.47
7	6	0	14.22	-14.71
2	11	0	6.08	6.32
8	3	0	21.37	18.80
4	10	0	32.19	-31.21
6	8	0	29.28	28.16
8	4	0	26.02	27.72
3	11	0	8.87	-5.52
7	7	0	10.48	-9.79
0	12	0	13.60	19.22
8	5	0	70.44	72.74
1	12	0	57.87	60.42
5	10	0	14.80	13.46
6	9	0	14.57	15.01
4	11	0	33.13	-34.06
2	12	0	38.93	40.07
9	1	0	5.85	-4.00
7	8	0	6.77	6.68
9	2	0	17.44	-14.67

TABLE A-1. (CONTINUED)

H	K	L	OBS	CALC
8	6	0	11.58	13.96
3	12	0	21.72	18.89
9	3	0	6.40	-9.04
6	10	0	15.77	21.11
5	11	0	8.23	3.19
9	4	0	19.87	22.46
8	7	0	8.06	-4.10
1	13	0	16.03	14.77
4	12	0	27.47	28.23
2	13	0	12.74	14.94
7	9	0	15.11	17.52
9	5	0	9.37	6.68
8	8	0	37.43	36.81
3	13	0	0.	1.99
10	0	0	4.27	3.08
9	6	0	32.41	30.12
10	1	0	23.11	-18.65
6	11	0	47.53	47.90
5	12	0	26.10	-25.57
7	10	0	15.44	-16.42
10	2	0	24.57	24.86
0	14	0	41.55	41.16
10	3	0	7.16	-2.60
1	14	0	8.50	4.91
4	13	0	7.73	13.93
9	7	0	0.	-5.22
8	9	0	32.25	33.14
2	14	0	64.68	-65.76
10	4	0	35.11	35.69
6	12	0	12.73	17.81
3	14	0	30.08	30.14
10	5	0	44.42	45.79
7	11	0	50.09	49.43
5	13	0	4.42	6.70
9	8	0	65.93	-67.28
8	10	0	27.18	27.01
10	6	0	39.47	-39.18
4	14	0	49.40	-53.40
1	15	0	33.18	-36.25
11	1	0	0.	6.28
2	15	0	10.55	12.74
11	2	0	29.24	29.68
9	9	0	0.	-3.61
7	12	0	5.65	-3.98
11	3	0	10.25	-8.32
6	13	0	18.44	16.99
10	7	0	70.62	-72.14
8	11	0	10.61	-12.76
3	15	0	16.50	15.90
5	14	0	36.41	36.51
11	4	0	22.56	23.26
10	8	0	3.96	2.30
9	10	0	35.63	39.53
11	5	0	7.00	0.62
4	15	0	12.45	-6.34
0	16	0	16.96	10.15
1	16	0	25.82	24.82
7	13	0	6.92	1.19
2	16	0	7.59	12.94
11	6	0	15.70	15.84
6	14	0	35.61	38.24
8	12	0	18.36	-15.19
10	9	0	2.25	-3.99
12	0	0	18.38	13.40
12	1	0	8.87	-6.22
5	15	0	31.72	-35.02
3	16	0	8.07	-5.67
9	11	0	50.65	-48.78
12	2	0	10.09	-15.93
11	7	0	23.38	-19.12
12	3	0	10.72	-3.47
4	16	0	37.35	40.52
12	4	0	8.63	-14.61
7	14	0	60.05	-62.08
10	10	0	33.34	-32.92
8	13	0	52.35	-57.91
1	17	0	63.95	67.30
11	8	0	13.58	-21.76
6	15	0	15.73	14.08
12	5	0	17.65	16.77
2	17	0	23.01	-24.85
9	12	0	27.48	-24.39
5	16	0	33.14	34.25
3	17	0	18.06	-27.52
12	6	0	2.07	-4.71
11	9	0	12.15	16.56
10	11	0	28.56	-33.81
8	14	0	17.14	-19.07
7	15	0	10.04	14.16
4	17	0	21.40	20.06
13	1	0	9.79	17.16
9	13	0	19.43	-20.85
13	2	0	26.16	-29.85
12	7	0	15.51	-14.45
6	16	0	17.98	-25.35
0	18	0	58.26	59.87

TABLE A-1. (CONTINUED)

H	K	L	OBS	CALC
			(H0L) DATA	
0	0	1	45.72	-48.66
2	0	0	35.82	-32.33
-2	0	1	39.22	36.70
2	0	1	76.79	80.23
0	0	2	9.87	-9.29
-2	0	2	8.33	-7.83
-4	0	1	31.33	28.47
4	0	0	36.00	-32.32
2	0	2	69.88	-65.49
-4	0	2	29.36	-26.36
-2	0	3	64.36	65.86
0	0	3	59.68	-60.20
4	0	1	87.83	-92.84
-4	0	3	74.91	-76.54
2	0	3	46.15	42.61
-2	0	4	82.04	-79.27
4	0	2	42.92	42.59
-6	0	1	7.14	-3.42
-6	0	2	5.46	2.23
0	0	4	48.77	51.21
-4	0	4	60.15	63.06
6	0	0	64.22	61.86
-6	0	3	40.68	35.56
6	0	1	86.55	-87.33
2	0	4	15.48	23.05
-6	0	4	35.32	-36.47
-2	0	5	74.28	76.92
4	0	3	20.50	21.82
-4	0	5	57.26	57.00
0	0	5	129.67	-136.39
6	0	2	86.23	-87.14
-8	0	2	59.49	55.07
-6	0	5	59.87	-59.97
-8	0	1	60.57	-58.63
-8	0	3	81.43	87.74
8	0	0	20.11	-15.68
4	0	4	90.45	-90.35
-8	0	4	72.78	-71.77
2	0	5	19.88	27.28
-2	0	6	30.47	-26.99
-4	0	6	73.69	75.29
6	0	3	15.32	-9.49
0	0	6	43.82	45.66
-6	0	6	56.49	59.39
8	0	1	60.07	60.92

H	K	L	OBS	CALC
-8	0	5	32.87	-37.44
4	0	5	5.29	-0.98
8	0	2	72.91	-70.36
-10	0	2	5.29	1.43
-10	0	3	21.30	-22.17
-4	0	7	18.93	19.08
2	0	6	52.34	-48.01
-8	0	6	30.13	22.04
-2	0	7	22.03	16.95
-10	0	1	21.46	-18.70
6	0	4	18.48	15.50
-10	0	4	45.21	-41.83
10	0	0	5.23	3.08
-6	0	7	43.76	41.17
0	0	7	8.25	-6.03
-10	0	5	52.73	-52.41
8	0	3	13.38	-11.67
-8	0	7	29.45	-25.72
10	0	1	39.35	33.96
4	0	6	49.96	47.80
-10	0	6	19.15	-25.96
-4	0	8	37.31	34.22
6	0	5	36.87	-35.01
2	0	7	17.95	14.22
-2	0	8	46.64	-39.07
-6	0	8	15.84	-13.69
-12	0	3	67.17	64.00
10	0	2	26.91	29.22
8	0	4	88.82	83.48
-12	0	2	14.86	3.52
-12	0	4	11.57	-14.54
0	0	8	16.32	2.06
-10	0	7	35.69	29.79
-8	0	8	5.65	-1.32
-12	0	1	8.43	-2.63
-12	0	5	36.78	-35.00
12	0	0	20.48	13.40
4	0	7	26.82	-24.20
6	0	6	94.84	92.91
-4	0	9	61.39	-59.19
-12	0	6	18.84	-27.10
10	0	3	5.05	-7.80
-6	0	9	52.43	52.81
2	0	8	61.15	-61.13
-2	0	9	53.95	51.44
-10	0	8	31.74	23.08
8	0	5	41.77	34.24
12	0	1	8.26	-9.48
-8	0	9	68.94	63.05

TABLE A-1. (CONTINUED)

H	K	L	OBS	CALC
-12	0	7	20.57	-23.65
0	0	9	74.23	-72.57
10	0	4	24.11	22.55
-14	0	3	3.45	-6.02
-14	0	4	44.49	50.85
12	0	2	34.16	-45.30
-14	0	2	53.18	51.44
-10	0	9	4.47	-3.11
6	0	7	46.08	37.89
-14	0	5	54.69	50.31
4	0	8	38.44	-31.41
-12	0	8	10.88	-5.83
-4	0	10	26.31	-24.19
-6	0	10	5.70	-5.59
-14	0	1	52.72	-53.83
8	0	6	53.27	-59.34
-14	0	6	7.65	10.30
2	0	9	24.99	-33.23
-2	0	10	78.51	-79.04
-8	0	10	5.40	20.27
14	0	0	9.69	-10.64
12	0	3	66.76	68.15
-14	0	7	99.73	-103.48
10	0	5	16.19	13.42
-12	0	9	45.39	45.06
0	0	10	32.02	34.00

TABLE A-2. LOW TEMPERATURE OBSERVED AND CALCULATED STRUCTURE FACTORS. DATA ARE LISTED IN ORDER OF INCREASING BRAGG ANGLE.

H	K	L	OBS	CALC	ALPHA	H	K	L	OBS	CALC	ALPHA
(HKO) DATA						6	2	0	51.79	51.02	5
						5	5	0	30.40	30.43	81
1	1	0	19.17	18.23	97	6	3	0	40.02	40.18	6
0	2	0	89.75	81.86	178	4	7	0	8.54	13.80	-157
1	2	0	45.94	45.76	-81	3	8	0	26.54	26.42	-95
2	0	0	32.22	32.37	0	1	9	0	57.51	57.25	-81
2	1	0	12.11	12.81	-12	5	6	0	18.77	17.35	-69
1	3	0	18.19	17.11	-112	6	4	0	26.83	26.05	-151
2	2	0	40.74	40.19	11	2	9	0	26.58	28.63	168
0	4	0	23.09	24.68	9	6	5	0	9.07	6.76	59
3	0	0	6.88	5.44	0	7	0	0	10.76	10.76	0
2	3	0	42.14	42.09	11	7	1	0	32.51	32.10	91
1	4	0	4.59	4.94	-95	4	8	0	8.29	10.14	-68
3	1	0	8.82	8.82	-67	5	7	0	8.58	7.13	-174
3	2	0	10.48	8.19	75	7	2	0	46.44	46.15	98
2	4	0	8.99	6.56	37	3	9	0	3.63	8.10	62
3	3	0	51.04	50.71	81	0	10	0	93.36	93.35	-167
1	5	0	10.43	11.09	-143	7	3	0	39.53	39.03	-88
4	0	0	32.19	31.25	-0	1	10	0	14.92	13.36	93
4	1	0	14.82	16.79	-8	6	6	0	47.28	48.16	5
2	5	0	93.67	95.59	3	2	10	0	7.15	11.82	1
3	4	0	33.69	34.06	106	7	4	0	62.93	62.20	-67
4	2	0	9.82	8.29	138	5	8	0	14.01	14.75	-26
0	6	0	26.99	27.61	-152	4	9	0	19.08	19.50	-12
1	6	0	6.31	7.01	-27	6	7	0	22.85	26.27	24
4	3	0	1.57	7.53	126	3	10	0	59.83	58.84	-75
3	5	0	55.55	55.65	-76	7	5	0	60.29	59.78	92
2	6	0	43.30	42.68	-174	8	0	0	17.16	17.68	-0
4	4	0	5.73	10.22	121	8	1	0	30.44	30.51	4
5	0	0	6.51	1.70	-0	1	11	0	10.90	7.59	133
5	1	0	29.28	28.22	86	8	2	0	28.08	28.65	-16
1	7	0	0.	4.97	-170	5	9	0	62.26	61.53	92
5	2	0	22.83	21.98	76	7	6	0	12.03	17.95	68
3	6	0	19.37	20.61	-100	2	11	0	4.78	9.43	-76
4	5	0	61.51	60.83	19	8	3	0	24.49	24.41	36
5	3	0	36.69	37.32	69	4	10	0	32.47	33.09	-150
2	7	0	19.78	18.92	47	6	8	0	28.19	27.35	-165
5	4	0	11.83	12.23	-105	8	4	0	27.49	27.09	-15
0	8	0	60.77	60.31	-153	3	11	0	9.23	14.28	45
1	8	0	42.03	41.88	86	7	7	0	7.89	7.38	101
3	7	0	27.61	27.84	-94	0	12	0	15.45	13.87	-17
4	6	0	48.68	48.68	176	8	5	0	72.12	72.03	12
6	0	0	62.25	62.15	0	1	12	0	58.14	58.36	100
6	1	0	21.35	20.87	-12	5	10	0	14.59	13.79	98
2	8	0	31.18	31.83	-157	6	9	0	13.35	18.10	-163

TABLE A-2. (CONTINUED)

H	K	L	OBS	CALC	ALPHA
4	11	0	32.61	31.86	-149
2	12	0	39.36	38.97	-160
9	0	0	9.31	5.67	-0
9	1	0	11.12	8.32	6
9	2	0	21.11	19.87	-13
3	12	0	23.13	24.59	-4
6	10	0	14.85	17.22	-148
9	4	0	17.36	19.90	78
1	13	0	11.81	11.42	85
7	9	0	14.50	15.85	-105
4	12	0	30.74	31.21	9
2	13	0	11.29	12.94	150
8	8	0	38.84	38.80	26
9	6	0	31.30	30.12	67
10	1	0	20.68	23.03	31
5	12	0	25.62	26.04	-81
7	10	0	13.80	17.20	107
10	2	0	24.47	25.13	164
0	14	0	42.64	44.06	-13
8	9	0	35.02	34.31	14
2	14	0	65.37	64.89	24
10	4	0	34.63	35.88	154
3	14	0	30.02	31.24	-101
10	5	0	42.82	43.80	175
7	11	0	49.84	49.23	-78
9	8	0	66.30	66.93	-89
8	10	0	27.54	26.74	-2
10	6	0	38.10	38.35	8
4	14	0	48.24	49.02	-173
1	15	0	31.21	33.27	-87
11	0	0	0.	0.72	0
11	2	0	27.08	26.76	-82
10	7	0	72.54	72.66	25
5	14	0	35.79	35.27	84
9	10	0	34.23	34.82	100
0	16	0	15.67	13.64	87
1	16	0	26.77	26.65	137
5	15	0	31.44	32.61	-52
9	11	0	49.04	48.67	-71
11	7	0	22.48	20.97	79
4	16	0	34.50	37.40	27
7	14	0	61.55	60.76	109
10	10	0	31.23	29.36	-9
8	13	0	51.43	50.67	-145
1	17	0	63.48	62.89	115
2	17	0	20.12	22.65	19
9	12	0	22.39	24.23	-90
5	16	0	30.76	31.73	125
10	11	0	29.12	30.39	22
13	2	0	27.11	28.20	-92
0	18	0	59.36	58.48	24

(H0L) DATA

H	K	L	OBS	CALC
0	0	1	45.13	-48.76
-1	0	1	6.60	5.36
2	0	0	35.59	32.37
1	0	1	7.04	-6.77
-2	0	1	39.55	-36.20
-1	0	2	7.59	-15.29
2	0	1	73.53	-80.18
-3	0	1	9.60	-3.11
0	0	2	10.93	-7.36
-2	0	2	8.96	8.45
3	0	0	7.25	5.44
1	0	2	5.21	2.89
-3	0	2	12.36	16.42
3	0	1	10.62	-7.09
-4	0	1	32.38	26.40
4	0	0	36.26	-31.25
2	0	2	68.45	65.15
-4	0	2	29.21	-28.61
-1	0	3	8.82	-6.75
-2	0	3	63.58	-63.68
0	0	3	60.71	-62.07
-3	0	3	9.00	13.48
4	0	1	85.83	-98.13
-5	0	1	5.58	-24.36
1	0	3	7.15	11.93
-4	0	3	73.42	-75.54
3	0	2	9.96	-9.53
-5	0	2	9.34	9.23
5	0	0	9.01	-1.70
2	0	3	46.42	-44.90
-5	0	3	9.20	8.75
-2	0	4	81.50	81.22
-1	0	4	9.71	13.50
-3	0	4	11.92	-8.44
5	0	1	11.44	10.85
4	0	2	43.56	38.67
-6	0	1	9.10	2.73
-6	0	2	9.36	0.11
0	0	4	48.41	50.30
-4	0	4	58.87	62.20
6	0	0	64.00	-62.15
3	0	3	14.08	-13.70

ABLE A-2. (CONTINUED)

H	K	L	OBS	CALC
-6	0	3	39.10	-35.26
1	0	4	4.76	22.03
-5	0	4	4.76	-12.48
5	0	2	9.66	-3.95
-7	0	2	8.35	1.52
6	0	1	85.42	87.05
-7	0	1	11.03	11.11
2	0	4	17.24	-19.63
-6	0	4	34.81	35.57
-2	0	5	71.64	-73.86
-3	0	5	8.67	5.34
4	0	3	21.95	27.11
-7	0	3	8.12	11.01
-1	0	5	7.84	0.13
-4	0	5	57.49	55.47
7	0	0	15.12	-10.76
0	0	5	125.24	-128.67
-5	0	5	13.67	12.19
3	0	4	6.92	-10.52
-7	0	4	4.89	17.69
6	0	2	84.93	84.91
-8	0	2	57.97	54.63
1	0	5	5.37	-6.08
-6	0	5	56.89	57.65
7	0	1	5.37	-9.34
-8	0	1	58.79	-59.89
5	0	3	6.21	-1.58
-8	0	3	79.94	85.14
8	0	0	19.15	-17.68
4	0	4	91.65	-88.55
-3	0	6	6.60	12.64
2	0	5	18.89	-29.09
-8	0	4	70.15	-66.81
-7	0	5	5.82	9.93
-2	0	6	28.15	28.43
-4	0	6	72.58	75.42
-1	0	6	5.82	6.58
-5	0	6	5.39	-0.72
7	0	2	5.38	-15.12
-9	0	2	5.82	0.79
6	0	3	16.51	6.57
-9	0	3	9.06	-11.86
8	0	1	61.29	58.39
0	0	6	45.06	45.87
-9	0	1	9.59	28.75
-6	0	6	56.95	-55.09
3	0	5	9.83	-15.63
-8	0	5	33.11	-37.72
5	0	4	10.98	-5.59
-9	0	4	9.04	-10.66
1	0	6	10.28	0.80
9	0	0	12.79	-5.67
-7	0	6	17.42	-18.87
4	0	5	7.85	-8.35
8	0	2	73.15	-72.38
-9	0	5	13.78	-2.80
7	0	3	11.32	5.52
-10	0	2	6.88	-1.05
-10	0	3	23.15	20.33
-3	0	7	8.42	-7.89
-4	0	7	17.17	19.73
2	0	6	52.90	43.44
-8	0	6	27.17	23.06
-2	0	7	21.26	-17.00
-5	0	7	7.19	-10.51
9	0	1	5.73	13.11
-10	0	1	22.33	23.04
6	0	4	28.43	-20.88
-10	0	4	48.03	44.94
-1	0	7	11.43	2.76
-6	0	7	50.45	-39.41
10	0	0	20.64	0.81
0	0	7	7.41	-8.19
3	0	6	5.25	10.50
5	0	5	10.48	-7.09
-7	0	7	11.71	2.59
-9	0	6	11.51	-10.05
-10	0	5	56.73	47.21
8	0	3	18.05	-11.43
-11	0	3	9.94	-7.33
9	0	2	9.94	9.25
-11	0	2	13.24	9.12
1	0	7	6.68	0.50
-8	0	7	29.44	-24.79
7	0	4	17.17	9.74
-11	0	4	8.15	-18.31
10	0	1	39.92	-35.44
-11	0	1	5.55	10.80
4	0	6	53.36	51.86
-10	0	6	20.22	28.87
-4	0	8	36.51	34.40
-3	0	8	11.76	-1.28
6	0	5	37.88	32.93
-5	0	8	5.88	13.33
-2	0	8	47.10	39.98
-12	0	3	63.34	59.65
8	0	4	88.26	74.98
-10	0	7	31.63	-30.90

TABLE A-2. (CONTINUED)

H	K	L	OBS	CALC
-12	0	5	34.23	-33.51
1	0	8	8.53	3.18
6	0	6	98.10	-92.00
-4	0	9	60.19	-56.87
-6	0	9	52.90	-47.75
9	0	4	7.12	-20.16
2	0	8	61.13	62.58
-2	0	9	55.42	-49.62
8	0	5	42.67	34.23
-8	0	9	66.80	60.65
7	0	6	5.39	-11.93
-13	0	6	6.67	6.75
0	0	9	73.24	-68.31
13	0	0	7.67	12.83
-14	0	4	45.09	-46.35
12	0	2	37.45	-40.76
-14	0	2	55.20	-45.75
9	0	5	12.11	11.52
6	0	7	49.94	-39.29
-14	0	5	55.27	-47.94
4	0	8	44.43	-37.62
-13	0	7	12.47	14.90
-14	0	1	54.85	52.81
-3	0	10	9.16	20.44
8	0	6	56.88	-58.53
-2	0	10	79.33	77.95
12	0	3	73.89	61.55
-11	0	9	16.46	17.08
-14	0	7	94.21	95.06
3	0	9	4.24	-1.72
-12	0	9	45.37	37.57
0	0	10	42.77	34.29